UNITED STATES AIR FORCE

AIR UNIVERSITY

AIR FORCE INSTITUTE OF TECHNOLOGY

Wright-Patterson Air Force Base, Ohio

Unclassified

Security Classification

DOCUMENT CONTROL DATA - R & D

(Security classification of title, body of abstract and indexing annotation must be entered when the overall report is classified)

1 ORIGINATING ACTIVITY (Corporate author)

Air Force Institute of Technology
Wright-Patterson AFB, Ohio 45433

2a. REPORT SECURITY CLASSIFICATION

Unclassified

2b GROUP

3 REPORT TITLE

PURSUIT-EVASION GAMES BETWEEN TWO SPACECRAFT IN NEAR-EARTH ORBIT

4 DESCRIPTIVE NOTES (Type of report and inclusive dates)

AFIT Thesis

5 AUTHOR(S) (First name, middle initial, last name)

Richard H. Woodward
Captain USAF

6 REPORT DATE	7a TOTAL NO OF PAGES	7b NO OF REFS
March 1972	115	4

8a CONTRACT OR GRANT NO	9a. ORIGINATOR'S REPORT NUMBER(S)
b. PROJECT NO N/A	GA/MC/72-7
c.	9b OTHER REPORT NO(S) (Any other numbers that may be assigned this report)
d.	

10 DISTRIBUTION STATEMENT

Approved for public release; distribution unlimited.

Approved for public release; IAW AFR 190-17

Keith A. Williams, 1st Lt., USAF
Assistant Director of Information, AFIT

11 SUPPLEMENTARY NOTES

12 SPONSORING MILITARY ACTIVITY

13 ABSTRACT

This paper considers the problem of developing the optimum thrust angle programs for two constant mass, constant thrust spacecraft engaged in pursuit and evasion in near-earth orbit. The problem is formulated as a differential game in which the pursuer attempts to minimize the final separation distance while the evader attempts to maximize it.

The problem is approached by linearizing the equations of motion about a circular reference orbit at the earth's surface. The validity of the linearized equations is verified by comparing a linearized trajectory to six non-linear trajectories. Optimum non-linear trajectories are generated by backward integration. The fixed-time and free-time two point boundary value problems are solved for the linear case. It is found that convergence to a free-time solution becomes exceedingly difficult if the flight time is short.

A pseudo closed loop control law is developed and tested numerically against two non-optimum evaders. The results of this control law test are promising but further tests are warranted due to the limited number of cases considered.

DD FORM 1 NOV 68 1473

Unclassified

14 KEY WORDS	LINK A		LINK B		LINK C	
	ROLE	WT	ROLE	WT	ROLE	WT
Differential Games						
Pursuit-Evasion						
Trajectory Optimization						
Near-Earth Orbit						
End Game						
Fixed-Time Two Point Boundary Value Problem						
Free-Time Two Point Boundary Value Problem						

PURSUIT-EVASION GAMES BETWEEN TWO SPACECRAFT IN NEAR-EARTH ORBIT

THESIS

GA/MC/72-7 Richard H. Woodward
Captain USAF

Approved for public release; distribution unlimited.

GA/MC/72-7

PURSUIT-EVASION GAMES BETWEEN TWO SPACECRAFT IN NEAR-EARTH ORBIT

THESIS

Presented to the Faculty of the School of Engineering of
the Air Force Institute of Technology
Air Univeristy
in Partial Fulfillment of the
Requirements for the Degree of
Master of Science

by

Richard H. Woodward, B.S.A.E.
Captain USAF
Graduate Astronautics

March 1972

Preface

This work represents the outcome of my attempt to formulate and solve a two spacecraft encounter viewed as a differential game. The vehicles are constrained to maneuver in only two dimensions, but the gravity field is allowed to vary as a function of altitude. Much of the work centers around pseudo linearized equations of motion.

I wish to express my appreciation to the faculty members of the Air Force Institute of Technology who have either influenced or assisted me in this effort. In particular, I am indebted to Prof. Gerald M. Anderson for introducing me to the field of optimization theory and for guiding my thesis effort.

Richard H. Woodward

Contents

List of Figures

List of Tables

List of Symbols

Symbol	Definition
d	actual separation distance between pursuer and evader
D	normalized separation distance between pursuer and evader
F	coefficient matrix of Y state variables
G	control matrix
H	Hamiltonian function
J	cost or payoff function
m	mass
P	costates of Y
r	radius from Earth's center
r_0	radius of spherical Earth's surface
t	time
T	thrust
u	normalized thrust $u = \frac{r_0 T}{m V_0^2}$
V_0	velocity of circular orbit at Earth's surface
V_r	radial velocity
V_θ	transverse velocity
x	state variable for single spacecraft
Y	relative difference state variable
Y_0	initial, assumed measurable, state
α	thrust (control) angle measured positive upward from the local horizontal
θ	angular position of spacecraft in orbital plane measured in the direction of motion and from some arbitrary fixed reference

Symbol	Definition
λ	costates of x
μ	Earth's gravitational constant
τ	characteristic time $\tau = \frac{V_0 t}{r_0}$
τ_0	initial characteristic time
ϕ	individual element in transition matrix
Φ	transition or fundamental matrix

Superscripts

$\dot{}$	denotes derivative with respect to time
$'$	denotes derivative with respect to characteristic time (τ)

Subscripts

E	denotes evader
f	denotes final (end) condition
P	denotes pursuer

Abstract

This paper considers the problem of developing the optimum thrust angle programs for two constant mass, constant thrust spacecraft engaged in pursuit and evasion in near-earth orbit. The problem is formulated as a differential game in which the pursuer attempts to minimize the final separation distance while the evader attempts to maximize it.

The problem is approached by linearizing the equations of motion about a circular reference orbit at the earth's surface. The validity of the linearized equations is verified by comparing a linearized trajectory to six non-linear trajectories. Optimum non-linear trajectories are generated by backward integration. The fixed-time and free-time two point boundary value problems are solved for the linear case. It is found that convergence to a free-time solution becomes exceedingly difficult if the flight time is short.

A pseudo closed loop control law is developed and tested numerically against two non-optimum evaders. The results of this control law test are promising but further tests are warranted due to the limited number of cases considered.

PURSUIT-EVASION GAMES BETWEEN TWO SPACECRAFT IN NEAR-EARTH ORBIT

I. Introduction

Background

The advent of viable military space systems by potentially agressive foreign powers has raised the possibility of our country's earth satellites coming under hostile attack. Such a possibility has prompted a need for an investigation to determine the optimum methods of avoiding destruction or capture in the event of such an encounter.

Problem

This study analyzes the pursuit-evasion situation through the use of differential game theory. The specific situation investigated is the two dimensional (planar) problem in near-earth orbit with the final separation distance between the two vehicles being the zero sum payoff. Both the fixed and free-time problems are discussed.

Current Knowledge

There has been much successful work over the last decade using differential games to investigate aircraft pursuit-evasion problems. However, there have been but relatively few attempts to utilize this game technique in the study of orbital problems. Billik (Ref 2) used differential games to solve the minimum energy, fixed-time problem in an inverse square gravity field. Wong (Ref 4) used the

same technique to investigate the fixed-time, minimum final separation, assuming that the encounter took place in a region where gravity was constant. To date, there apparently have been no published solutions to the minimum distance, free-time problem in an inverse square gravity field. The absence of solutions is probably due to the complications which arise primarily due to the free-time aspect of the problem.

Scope

This thesis will consider the minimum distance, fixed and free-time problems in an inverse square gravity field. This study will consider only the end game, that is, the situation after the pursuer has closed to within about 100 nautical miles of the evader and is continuing to close. This magnitude of distance has been selected as a maximum range for an on-board radar system. Not considered will be any action on the part of either vehicle before that situation is reached, that is, gross rendezvous will not be considered. Also, this thesis will consider the formulation of both open loop and closed loop control laws.

Assumptions

The assumptions to be made follow. Where applicable, a brief explanation is offered.

1. Free time. The overall objective is to solve the free-time problem as it is felt that this is a more realistic situation than constraining the time of game termination.

However, in the course of obtaining free-time solutions, fixed-time solutions are a natural stepping stone. The fixed-time solutions are also important in their own right and are useful for modeling certain scenarios, such as limited fuel cases.

2. Inverse square gravity field.

3. Both vehicles thrust continuously. Once either vehicle discontinued thrusting, the situation could from that point on no longer be considered a two player game. If the pursuer ceased thrusting, the evader would then have a simple avoidance problem. If the evader quit thrusting, the pursuer would have a simple intercept or rendezvous problem. The latter situation has already received considerable attention.

4. The thrust magnitude of each vehicle is fixed. Even with variable thrust engines, the players would find it most advantageous to use maximum thrust for maximum control.

5. Control is provided by varying the direction of thrust.

6. Payoff will be the separation distance at problem termination. For the free-time problem, this will be at the point of closest approach. The effectiveness of the pursuer will be related to how close he can get to the evader. The evader, on the other hand, will desire to maximize that separation distance.

7. Perfect information. Each vehicle will be aware of

the current state and capabilities of both vehicles.

8. Fixed mass. This eliminates one area of extreme complications which could be a study in itself. This assumption is a good approximation when considering low thrust and relatively short burn durations. In addition, the larger the vehicle, the less is the introduced error.

9. No barriers or ill-defined surfaces. That is, it will be assumed that the solution in the small is valid.

Approach

1. Linearize the equations of motion about a circular reference orbit.

2. Set up appropriate equations for a differential game formulation of both the linear and non-linear equations.

3. Apply the necessary conditions for the optimal minimax solution as dictated by general optimization techniques.

4. Compare an open loop linear trajectory to open loop non-linear trajectories to check the validity of the linearized formulation with respect to the end conditions.

5. Solve the linear fixed-time two point boundary value problem (TPBVP) by using sets of initial conditions obtained from the open loop non-linear trajectories. This will allow comparison of the linear and non-linear trajectories with respect to the initial conditions.

6. Extend the TPBVP solution to the free-time case.

7. Develop and test a form of a near-optimal closed loop control law for the optimal trajectory.

II. General Equations

Non-linear Equations of Motion

Almost any text on dynamics can be consulted for the general equations for two dimensional orbital motion. They are as follows:

$$\ddot{r} - r\dot{\theta}^2 = \frac{-\mu}{r^2} + \frac{T \sin \alpha}{m} \tag{1}$$

$$r\ddot{\theta} + 2\dot{r}\dot{\theta} = \frac{T \cos \alpha}{m} \tag{2}$$

Where as shown in Fig. 1, α is measured from the local horizontal. It is desirable to have these equations in terms of the radial and transverse velocities, V_r and V_θ respectively, where

$$V_r = \dot{r} \tag{3a}$$

and

$$V_\theta = r\dot{\theta} \tag{3b}$$

Making use of these velocities, we can replace the terms in Eqs (1) and (2) involving $\dot{r}$, $\ddot{r}$, $\dot{\theta}$ and $\ddot{\theta}$ to yield

$$\dot{V}_r - \frac{V_\theta^2}{r} = \frac{-\mu}{r^2} + \frac{T \sin \alpha}{m} \tag{4a}$$

$$\dot{V}_\theta + \frac{V_r V_\theta}{r} = \frac{T \cos \alpha}{m} \tag{4b}$$

The above are the non-linear equations of motion.

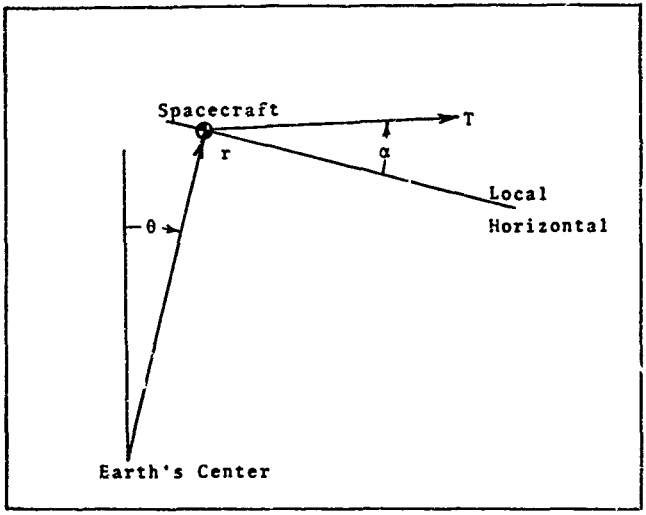

Fig. 1. Orbital Geometry.

Linearized Equations of Motion

Linearization of Eqs (3) and (4) yield

$$\Delta\dot{r} = \Delta V_r \tag{5a}$$

$$\Delta\dot{\theta} = \frac{\Delta V_\theta}{r} - \frac{V_\theta \Delta r}{r^2} \tag{5b}$$

$$\Delta\dot{V}_r - \frac{2V_\theta \Delta V_\theta}{r} + \left(\frac{V_\theta^2}{r^2} - \frac{2\mu}{r^3}\right)\Delta r = \frac{T \sin\alpha}{m} \tag{6}$$

and

$$\Delta\dot{V}_\theta + \frac{V_r \Delta V_\theta}{r} + \frac{V_\theta \Delta V_r}{r} - \frac{V_r V_\theta \Delta r}{r^2} = \frac{T \cos\alpha}{m} \tag{7}$$

where now r, V_θ and V_r refer to some reference orbit and the delta quantities refer to deviations from that reference orbit. Letting the reference orbit be circular allows the following simplifications:

$$V_r = 0$$

and

$$r\dot{\theta}^2 = \frac{\mu}{r^2}$$

or

$$\frac{V_\theta^2}{r} = \frac{\mu}{r^2}$$

Using the above in Eqs (6) and (7) yields

$$\Delta\dot{V}_r = \frac{2V_\theta \Delta V_\theta}{r} + \frac{V_\theta^2 \Delta r}{r^2} + \frac{T \sin \alpha}{m} \qquad (8a)$$

$$\Delta\dot{V}_\theta = -\frac{V_\theta \Delta V_r}{r} + \frac{T \cos \alpha}{m} \qquad (8b)$$

Equations (5) and (8) are now the linearized equations of motion.

Non-linear Separation

Figure 2 illustrates the geometry involved with determining the separation distance between two orbital vehicles, hereafter called a pursuer (P) and an evader (E).

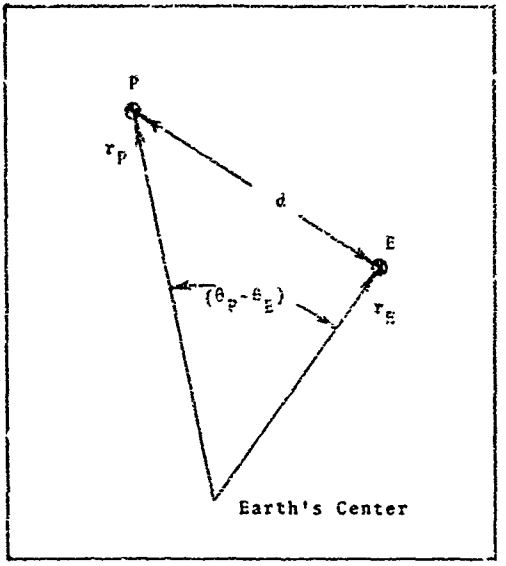

Fig. 2. Non-linear Separation.

From the law of cosines,

$$d^2 = r_E^2 + r_p^2 - 2r_E r_p \cos(\theta_p - \theta_E) \qquad (9)$$

Separation in Linearized Coordinates

Figure 3 illustrates the same geometry as related to a reference orbit. Again from the law of cosines

$$d^2 = (r + \Delta r_p)^2 + (r + \Delta r_E)^2 -$$

$$- 2(r + \Delta r_p)(r + \Delta r_E) \cos(\Delta\theta_p - \Delta\theta_E) \qquad (10)$$

By expanding Eq (10) in a Taylor series and eliminating

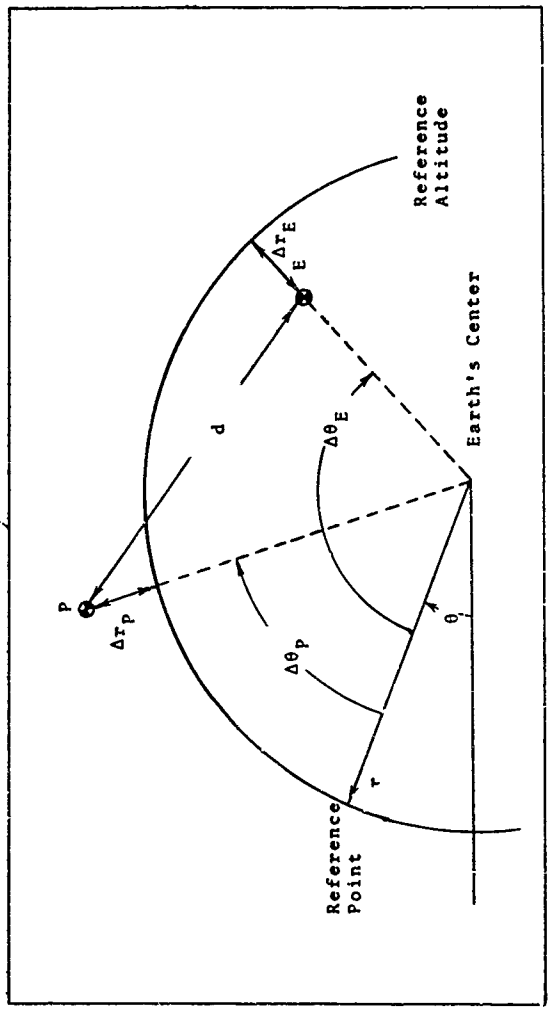

Fig. 3. Linear Separation.

higher order terms on the assumption that $\Delta r << r$, the following is obtained.

$$d^2 = (\Delta r_p - \Delta r_E)^2 + r^2(\Delta\theta_p - \Delta\theta_E)^2 \qquad (11)$$

Normalized Equations

It should be noted that the numerical values of parameters such as r and V will differ by several orders of magnitude. That is, V may be several miles per second while r may be several thousand miles. Because of this computation that involves both parameters may result in information being lost due to a lack of significant digits. To avoid this, it is desirable to normalize the equations of interest so that all parameters will be of the same order of magnitude.

This author, like so many before him chose to normalize the equations with respect to a circular orbit at the surface of a spherical earth. Thus, distances become normalized by r_0, the radius of the earth surface orbit, while the velocities become normalized by V_0, the transverse orbital velocity of that circular orbit.

The use of a circular orbit allows one to simplify the gravitational constant μ. Since μ equals the product of any circular orbit's velocity squared and that circular orbit's radius, the use of a circular orbit allows the value of μ to be replaced by simply unity.

It should immediately be pointed out that the normalization is not without its drawback. The unit of time must also become non-dimensional. Thus, introduce a non-dimensional characteristic time unit

$$\tau = \frac{V_0 t}{r_0} \tag{12}$$

This will necessitate changing the time derivatives to tau derivatives by use of the chain rule for differentiation.

$$\frac{d(\ )}{d\tau} = \frac{d(\ )}{dt}\frac{dt}{d\tau} = \frac{r_0}{V_0}\frac{d(\ )}{dt} \tag{13}$$

Since differentiation with respect to time is indicated by a dot, differentiation with respect to tau will be denoted by a prime, hence

$$\frac{dV_r}{d\tau} = V_r'$$

Non-linear Normalization

Using the aforementioned procedure, it is now possible to normalize the non-linear equations. First define the following normalized state variables.

$$x_1 = \frac{r}{r_0} \tag{14a}$$

$$x_2 = \frac{V_r}{V_0} \tag{14b}$$

$$x_3 = \theta \tag{14c}$$

$$x_4 = \frac{V_\theta}{V_0} \tag{14d}$$

Then making use of Eq (13),

$$x_1' = x_2 \tag{15a}$$

Likewise,

$$\frac{dx_2}{d\tau} = \frac{r_0}{V_0}\frac{dx_2}{dt}$$

$$= \frac{r_0}{V_0}\quad\frac{1}{V_0}\quad\left[\frac{V_\theta^2}{r} - \frac{\mu}{r^2} + \frac{T \sin \alpha}{m}\right]$$

$$= \frac{x_4^2}{x_1} - \frac{1}{x_1^2} + \frac{r_0 T \sin \alpha}{V_0^2 m}$$

By defining

$$u = \frac{r_0 T}{V_0^2 m}$$

where both T (thrust) and m (mass) remain constant, the last equation can be written as

$$x_2' = \frac{x_4^2}{x_1} - \frac{1}{x_1^2} + u \sin \alpha \tag{15b}$$

Equations (3b) and (13) yield

$$x_3' = \frac{x_4}{x_1} \tag{15c}$$

Finally,

$$x_4' = -\frac{x_2 x_4}{x_1} + u \cos \alpha \tag{15d}$$

Equations (15) now are the normalized, non-linear state equations. The square of the non-linear separation, Eq (9), can also be normalized. Let the result be called D^2.

$$D^2 = x_{1E}^2 + x_{1P}^2 - 2x_{1E}x_{1P} \cos (x_{3P} - x_{3E}) \tag{16}$$

Linearized Equations

Using the same procedure, it is possible to normalize the linear equations. Define the following normalized linear state variables.

$$\Delta x_1 = \frac{\Delta r}{r_0} \tag{17a}$$

$$\Delta x_2 = \frac{\Delta V_r}{V_0} \tag{17b}$$

$$\Delta x_3 = \Delta\theta \tag{17c}$$

$$\Delta x_4 = \frac{\Delta V_\theta}{V_0} \tag{17d}$$

Now making use of Eq (13) and the linear equations, the state equations can be derived.

$$\Delta x_1' = \Delta x_2 \tag{18a}$$

$$\Delta x_2' = \frac{2V_\theta r_0 \Delta x_4}{V_0 r} + \frac{V_\theta^2 r_0^2 \Delta x_1}{V_0^2 r^2} + u \sin \alpha \tag{18b}$$

where u is again defined as $\frac{r_0 T}{V_0^2 m}$.

Also,

$$\Delta x_3' = \frac{r_0 \Delta x_4}{r} - \frac{r_0^2 V_\theta \Delta x_1}{r^2 V_0} \tag{18c}$$

and lastly,

$$\Delta x_4' = \frac{-r_0 V_\theta \Delta x_2}{r V_0} + u \cos \alpha \tag{18d}$$

Observation of Eqs (18) yields the conclusion that considerable simplification could be made if the reference orbit used for linearizing were identical to the orbit used for normalizing; i.e., $r = r_0$ and $V_\theta = V_0$. Making that very simplification, the following normalized, linearized state equations follow:

$$\Delta x_1' = \Delta x_2 \tag{19a}$$

$$\Delta x_2' = 2\Delta x_4 + \Delta x_1 + u \sin \alpha \tag{19b}$$

$$\Delta x_3' = \Delta x_4 - \Delta x_1 \tag{19c}$$

$$\Delta x_4' = -\Delta x_2 + u \cos \alpha \tag{19d}$$

As before, Eq (11) can also be normalized to yield

$$D^2 = (\Delta x_{1P} - \Delta x_{1E})^2 + (\Delta x_{3P} - \Delta x_{3E})^2 \tag{20}$$

It should be noted here that the state equations, Eq (19),are only linear in the states. Those equations are not linear in the control angle α. Thus, even though they will be referred to as linear equations, the reader should be aware of the non-linearity involved in the control function.

III. Differential Game Formulation

The formulation of the problems herein follows the standard pattern described in Bryson and Ho (Ref 2). The quantity to be minimaxed is the square of the final separation distance.

In the free-time problem, the final separation distance will be the minimum separation distance and the final time will thus occur at the point of closest approach. This separation distance at the point of closest approach is the quantity that the pursuer desires to minimize while the evader wishes to maximize it.

In the fixed-time problem, there are no assurances that the final separation distance will be the point of closest approach. However, if one would solve a large number of different fixed time problems, all with the same initial states, the final separation distance of one particular solution would be less than any of the others. That one particular fixed-time solution would then also be the free-time solution. Thus, the solution to the free-time problem is also the solution to one particular fixed-time problem. Hence, the technique used by this author to solve the free-time problem was simply to find that particular fixed-time solution whose final states corresponded to the point of closest approach.

For that reason, both the free and fixed-time two point boundary value problems will be presented here in linearized, normalized form, suitable for numerical solution. In addition, the non-linear normalized free-time two point boundary value problem will also be presented. The main purpose of the non-linear formulation is to serve as a comparison for the linear approximation formulations.

Non-linear Free-time TPBVP

The non-linear state equations, Eqs (15), plus the range squared expression, Eq (16), form the basis for this analysis. Both the pursuer (P) and evader (E) have identical state equations.

$$x'_{1P} = x_{2P} \tag{21a}$$

$$x'_{2P} = \frac{x_{4P}^2}{x_{1P}} - \frac{1}{x_{1P}^2} + u_P \sin \alpha_P \tag{21b}$$

$$x'_{3P} = \frac{x_{4P}}{x_{1P}} \tag{21c}$$

$$x'_{4P} = -\frac{x_{2P}x_{4P}}{x_{1P}} + u_P \cos \alpha_P \tag{21d}$$

$$x'_{1E} = x_{2E} \tag{22a}$$

$$x'_{2E} = \frac{x_{4E}^2}{x_{1E}} - \frac{1}{x_{1E}^2} + u_E \sin \alpha_E \tag{22b}$$

$$x'_{3E} = \frac{x_{4E}}{x_{1E}} \tag{22c}$$

$$x'_{4E} = -\frac{x_{2E}x_{4E}}{x_{1E}} + u_E \cos \alpha_E \tag{22d}$$

The payoff J becomes the normalized range squared expression, Eq (16), evaluated at the final time.

$$J = x_{1Ef}^2 + x_{1Pf}^2 - 2x_{1Ef}x_{1Pf} \cos (x_{3Pf} - x_{3Ef}) \tag{23}$$

The main equation, or Hamiltonian (H), can be formed by adjoining the costates to the state equations. Thus

$$\begin{aligned} H = {} & \lambda_{1P}x_{2P} + \lambda_{2P}\left[\frac{x_{4P}^2}{x_{1P}} - \frac{1}{x_{1P}^2} + u_P \sin \alpha_P\right] \\ & + \lambda_{3P}\frac{x_{4P}}{x_{1P}} + \lambda_{4P}\left[\frac{-x_{2P}x_{4P}}{x_{1P}} + u_P \cos \alpha_P\right] \\ & + \lambda_{1E}x_{2E} + \lambda_{2E}\left[\frac{x_{4E}^2}{x_{1E}} - \frac{1}{x_{1E}^2} + u_E \sin \alpha_E\right] \\ & + \lambda_{3E}\frac{x_{4E}}{x_{1E}} + \lambda_{4E}\left[-\frac{x_{2E}x_{4E}}{x_{1E}} + u_E \cos \alpha_E\right] \end{aligned} \tag{24}$$

Using the relationship $\lambda'_i = -\frac{\partial H}{\partial x_i}$, the costate differential equations can now be formed.

$$\lambda'_{1P} = \frac{1}{x_{1P}^2}\left[\lambda_{2P}\left(x_{4P}^2 - \frac{2}{x_{1P}}\right) + \lambda_{3P}x_{4P} - \lambda_{4P}x_{2P}x_{4P}\right] \quad (25a)$$

$$\lambda'_{2P} = -\lambda_{1P} + \frac{\lambda_{4P}x_{4P}}{x_{1P}} \quad (25b)$$

$$\lambda'_{3P} = 0 \quad (25c)$$

$$\lambda'_{4P} = -\frac{2\lambda_{2P}x_{4P}}{x_{1P}} - \frac{\lambda_{3P}}{x_{1P}} + \frac{\lambda_{4P}x_{2P}}{x_{1P}} \quad (25d)$$

$$\lambda'_{1E} = \frac{1}{x_{1E}^2}\left[\lambda_{2E}\left(x_{4E}^2 - \frac{2}{x_{1E}}\right) + \lambda_{3E}x_{4E} - \lambda_{4E}x_{2E}x_{4E}\right] \quad (26a)$$

$$\lambda'_{2E} = -\lambda_{1E} + \frac{\lambda_{4E}x_{4E}}{x_{1E}} \quad (26b)$$

$$\lambda'_{3E} = 0$$

$$\lambda'_{4E} = -\frac{2\lambda_{2E}x_{4E}}{x_{1E}} - \frac{\lambda_{3E}}{x_{1E}} + \frac{\lambda_{4E}x_{2E}}{x_{1E}} \quad (26d)$$

Also from the main equation, Eq (24), the optimum thrust angles can be found. Using the necessary condition that $\frac{\partial H}{\partial \alpha} = 0$,

$$\frac{\partial H}{\partial \alpha_p} = \lambda_{2P}u_P \cos \alpha_p - \lambda_{4P}u_P \sin \alpha_p$$

$$= 0$$

From which

$$\tan \alpha_p = \frac{\lambda_{2P}}{\lambda_{4P}}$$

That is, either

$$\sin \alpha_p = \frac{\lambda_{2P}}{\sqrt{\lambda_{2P}^2 + \lambda_{4P}^2}} \tag{27a}$$

and

$$\cos \alpha_p = \frac{\lambda_{4P}}{\sqrt{\lambda_{2P}^2 + \lambda_{4P}^2}} \tag{27b}$$

or

$$\sin \alpha_p = \frac{-\lambda_{2P}}{\sqrt{\lambda_{2P}^2 + \lambda_{4P}^2}} \tag{28a}$$

and

$$\cos \alpha_p = \frac{-\lambda_{4P}}{\sqrt{\lambda_{2P}^2 + \lambda_{4P}^2}} \tag{28b}$$

Likewise, it can be shown that

$$\tan \alpha_E = \frac{\lambda_{2E}}{\lambda_{4E}}$$

That is, either

$$\sin \alpha_E = \frac{\lambda_{2E}}{\sqrt{\lambda_{2E}^2 + \lambda_{4E}^2}} \tag{29a}$$

and

$$\cos \alpha_E = \frac{\lambda_{4E}}{\sqrt{\lambda_{2E}^2 + \lambda_{4E}^2}} \tag{29b}$$

or

$$\sin \alpha_E = \frac{-\lambda_{2E}}{\sqrt{\lambda_{2E}^2 + \lambda_{4E}^2}} \tag{30a}$$

and

$$\cos \alpha_E = \frac{-\lambda_{4E}}{\sqrt{\lambda_{2E}^2 + \lambda_{4E}^2}} \tag{30b}$$

The decision concerning which signs to use can be made by considering the sufficiency conditions. These are, for the pursuer $\frac{\partial^2 H}{\partial \alpha_p^2} > 0$ since he is attempting to minimize the cost and for the evader $\frac{\partial^2 H}{\partial \alpha_E^2} < 0$ since he is attempting to maximize the payoff. Thus, for the pursuer

$$\frac{\partial^2 H}{\partial \alpha_p^2} = -\lambda_{2p} u_p \sin \alpha_p - \lambda_{4p} u_p \cos \alpha_p$$

$$> 0 \tag{31}$$

It can be seen that to satisfy the pursuer's sufficiency condition, Eq (31), that the expressions with the minus signs, Eqs (28) must be the optimal solutions.

Now, for the evader,

$$\frac{\partial^2 H}{\partial \alpha_E^2} = - \lambda_{2E} u_E \sin \alpha_E - \lambda_{4E} u_E \cos \alpha_E$$

$$< 0 \qquad (32)$$

In this case, to satisfy the evader's sufficiency condition, the angle expressions with the plus signs must be chosen, Eqs (29).

Now, in an actual encounter, the initial states would be known, but the end states would not be known. The transversality conditions, however, would allow determination of the costates at the final time from the relation $\lambda_f = \frac{\partial J}{\partial x_f}$. These are as follows:

$$\lambda_{1Pf} = 2[x_{1Pf} - x_{1Ef} \cos (x_{3Pf} - x_{3Ef})] \qquad (33a)$$

$$\lambda_{2Pf} = 0 \qquad (33b)$$

$$\lambda_{3Pf} = 2[x_{1Ef} x_{1Pf} \sin (x_{3Pf} - x_{3Ef})] \qquad (33c)$$

$$\lambda_{4Pf} = 0 \qquad (33d)$$

$$\lambda_{1Ef} = 2[x_{1Ef} - x_{1Pf} \cos (x_{3Pf} - x_{3Ef})] \qquad (34a)$$

$$\lambda_{2Ef} = 0 \tag{34b}$$

$$\lambda_{3Ef} = -2x_{1Ef}x_{1Pf} \sin (x_{3Pf} - x_{3Ef}) \tag{34c}$$

$$\lambda_{4Ef} = 0 \tag{34d}$$

Since the cost is not a function of the final time, the transversality condition also gives the fact that $H(\tau_f) = 0$. In addition, since the Hamiltonian, Eq (24), is not an explicit function of time, then $H' = 0$ and thus for any point in time

$$H(\tau) = 0 \tag{35}$$

Hence, H must equal zero at the final time τ_f. Evaluating Eq (24) at τ_f and utilizing the transversality conditions, Eqs (33) and (34), for the costates yields

$$\begin{aligned} 0 = {} & x_{2Ef}x_{1Ef} + x_{2Pf}x_{1Pf} \\ & - (x_{2Ef}x_{1Pf} + x_{1Ef}x_{2Pf}) \cos (x_{3Pf} - x_{3Ef}) \\ & + (x_{1Ef}x_{4Pf} - x_{1Pf}x_{4Ef}) \sin (x_{3Pf} - x_{3Ef}) \end{aligned} \tag{36}$$

For this free-time formulation, the stopping condition occurs when the vehicles reach the point of closest approach. More formally, the problem would end when the range rate between the two vehicles reaches a zero value. This would also correspond to the point where the range squared rate

reaches zero. It has already been shown that the expression for range squared is

$$D^2 = x_{1E}^2 + x_{1P}^2 - 2x_{1E}x_{1P} \cos (x_{3P} - x_{3E}) \qquad (16)$$

This expression can be differentiated to yield an equation for range squared rate. Performing the differentiation yields

$$\begin{aligned} D^{2'} = {} & 2x_{1E}x'_{1E} + 2x_{1P}x'_{1P} - 2x'_{1E}x_{1P} \cos (x_{3P} - x_{3E}) \\ & - 2x_{1E}x'_{1P} \cos (x_{3P} - x_{3E}) + 2x_{1E}x_{1P}x'_{3P} \sin (x_{3P} - x_{3E}) \\ & - 2x_{1E}x_{1P}x'_{3E} \sin (x_{3P} - x_{3E}) \end{aligned} \qquad (37)$$

Substituting the appropriate state equations, Eqs (15), for the primed quantities in Eq (37) yields

$$\begin{aligned} D^{2'} = {} & 2x_{2E}x_{1E} + 2x_{2P}x_{1P} - 2x_{2E}x_{1P} \cos (x_{3P} - x_{3E}) \\ & - 2x_{1E}x_{2P} \cos (x_{3P} - x_{3E}) + 2x_{1E}x_{4P} \sin (x_{3P} - x_{3E}) \\ & - 2x_{1P}x_{4E} \sin (x_{3P} - x_{3E}) \\ = {} & 2[x_{2E}x_{1E} + x_{2P}x_{1P} - (x_{2E}x_{1P} + x_{1E}x_{2P}) \cos (x_{3P} - x_{3E}) \\ & + (x_{1E}x_{4P} - x_{1P}x_{4E}) \sin (x_{3P} - x_{3E})] \end{aligned} \qquad (38)$$

Note that if one sets Eq (38) equal to zero at the final time to form the appropriate stopping condition, the result is identically equal to the final Hamiltonian expression, Eq (36)! Thus, the stopping condition actually yields no additional information.

Thus, the non-linear, normalized, free-time two point boundary value problem consists of the state equations, Eqs (21) and (22), the costate equations, Eqs (25) and (26), the payoff, Eq (23), the Hamiltonian, Eq (24), the optimum control angles, Eqs (28) and (29), the transversality conditions, Eqs (33), (34) and (35) plus the initial values of the states.

Linear Free-time TPBVP

The linear state equations, Eqs (19), plus the range squared expression, Eq (20), form the basis for this formulation. As in the non-linear case, both the pursuer (P) and evader (E) have identical state equations.

$$\Delta x'_{1P} = \Delta x_{2P} \tag{39a}$$

$$\Delta x'_{2P} = 2\Delta x_{4P} + \Delta x_{1P} + u_P \sin \alpha_P \tag{39b}$$

$$\Delta x'_{3P} = \Delta x_{4P} - \Delta x_{1P} \tag{39c}$$

$$\Delta x'_{4P} = -\Delta x_{2P} + u_P \cos \alpha_P \tag{39d}$$

$$\Delta x'_{1E} = \Delta x_{2E} \tag{40a}$$

$$\Delta x'_{2E} = 2\Delta x_{4E} + \Delta x_{1E} + u_E \sin \alpha_E \tag{40b}$$

$$\Delta x'_{3E} = \Delta x_{4E} - \Delta x_{1E} \tag{40c}$$

$$\Delta x'_{4E} = -\Delta x_{2E} + u_E \cos \alpha_E \tag{40d}$$

The payoff, J, becomes the normalized, linearized range squared expression, Eq (20), evaluated at the final time:

$$J = (\Delta x_{1Pf} - \Delta x_{1Ef})^2 + (\Delta x_{3Pf} - \Delta x_{3Ef})^2 \tag{41}$$

The Hamiltonian becomes

$$\begin{aligned} H = {} & \Delta\lambda_{1P}\Delta x_{2P} + \Delta\lambda_{2P}(2\Delta x_{4P} + \Delta x_{1P} + u_P \sin \alpha_P) \\ & + \Delta\lambda_{3P}(\Delta x_{4P} - \Delta x_{1P}) + \Delta\lambda_{4P}(-\Delta x_{2P} + u_P \cos \alpha_P) \\ & + \Delta\lambda_{1E}\Delta x_{2E} + \Delta\lambda_{2E}(2\Delta x_{4E} + \Delta x_{1E} + u_E \sin \alpha_E) \\ & + \Delta\lambda_{3E}(\Delta x_{4E} - \Delta x_{1E}) + \Delta\lambda_{4E}(-\Delta x_{2E} + u_E \cos \alpha_E) \end{aligned} \tag{42}$$

Using Eq (42), the costate differential equations become

$$\Delta\lambda'_{1P} = -\Delta\lambda_{2P} + \Delta\lambda_{3P} \tag{43a}$$

$$\Delta\lambda'_{2P} = -\Delta\lambda_{1P} + \Delta\lambda_{4P} \tag{43b}$$

$$\Delta\lambda'_{3P} = 0 \tag{43c}$$

$$\Delta\lambda'_{4P} = -2\Delta\lambda_{2P} - \Delta\lambda_{3P} \tag{43d}$$

$$\Delta\lambda'_{1E} = -\Delta\lambda_{2E} + \Delta\lambda_{3E} \tag{44a}$$

$$\Delta\lambda'_{2E} = -\Delta\lambda_{1E} + \Delta\lambda_{4E} \tag{44b}$$

$$\Delta\lambda'_{3E} = 0 \tag{44c}$$

$$\Delta\lambda'_{4E} = -2\Delta\lambda_{2E} - \Delta\lambda_{3E} \tag{44d}$$

The optimum thrust angles can be found from the necessary conditions.

$$\frac{\partial H}{\partial \alpha_P} = 0$$

$$= \Delta\lambda_{2P}\, u_P \cos\alpha_P - \Delta\lambda_{4P}\, u_P \sin\alpha_P$$

From which,

$$\tan\alpha_P = \frac{\Delta\lambda_{2P}}{\Delta\lambda_{4P}}$$

As before, either

$$\sin\alpha_P = \frac{\Delta\lambda_{2P}}{\sqrt{\Delta\lambda_{2P}^2 + \Delta\lambda_{4P}^2}} \tag{45a}$$

and

$$\cos \alpha_p = \frac{\Delta\lambda_{4P}}{\sqrt{\Delta\lambda_{2P}^2 + \Delta\lambda_{4P}^2}} \tag{45b}$$

or

$$\sin \alpha_p = - \frac{\Delta\lambda_{2P}}{\sqrt{\Delta\lambda_{2P}^2 + \Delta\lambda_{4P}^2}} \tag{46a}$$

and

$$\cos \alpha_p = - \frac{\Delta\lambda_{4P}}{\sqrt{\Delta\lambda_{2P}^2 + \Delta\lambda_{4P}^2}} \tag{46b}$$

Likewise it can be shown that

$$\tan \alpha_E = \frac{\Delta\lambda_{2E}}{\Delta\lambda_{4E}}$$

where similar choices are available. Either

$$\sin \alpha_E = \frac{\Delta\lambda_{2E}}{\sqrt{\Delta\lambda_{2E}^2 + \Delta\lambda_{4E}^2}} \tag{47a}$$

and

$$\cos \alpha_E = \frac{\Delta\lambda_{4E}}{\sqrt{\Delta\lambda_{2E}^2 + \Delta\lambda_{4E}^2}} \tag{47b}$$

or

$$\sin \alpha_E = - \frac{\Delta\lambda_{2E}}{\sqrt{\Delta\lambda_{2E}^2 + \Delta\lambda_{4E}^2}} \tag{48a}$$

and

$$\cos \alpha_E = - \frac{\Delta\lambda_{4E}}{\sqrt{\Delta\lambda_{2E}^2 + \Delta\lambda_{4E}^2}} \tag{48b}$$

The correct signs are determined by the sufficiency conditions as was done before in Eqs (31) and (32). To satisfy those conditions, the pursuer's control must be described by Eqs (46), while the evader's optimum control must be described by Eqs (47).

It is assumed that the initial states are known, but the end states are not. Using the transversality conditions, the expressions for the costates at the final time can be determined in terms of the end states. These are as follows:

$$\Delta\lambda_{1Pf} = 2(\Delta x_{1Pf} - \Delta x_{1Ef}) \tag{48a}$$

$$\Delta\lambda_{2Pf} = 0 \tag{48b}$$

$$\Delta\lambda_{3Pf} = 2(\Delta x_{3Pf} - \Delta x_{3Ef}) \tag{48c}$$

$$\Delta\lambda_{4Pf} = 0 \tag{48d}$$

$$\Delta\lambda_{1Ef} = -2(\Delta x_{1Pf} - \Delta x_{1Ef}) \tag{49a}$$

$$\Delta\lambda_{2Ef} = 0 \tag{49b}$$

$$\Delta\lambda_{3Ef} = -2(\Delta x_{3Pf} - \Delta x_{3Ef}) \tag{49c}$$

$$\Delta\lambda_{4Ef} = 0 \tag{49d}$$

As in the non-linear case, neither the cost, Eq (41), nor the Hamiltonian, Eq (42), is an explicit function of time. Thus

$$H(\tau) = 0 \tag{50}$$

Evaluating the Hamiltonian, Eq (42), at the final time, utilizing the transversality conditions, Eqs (48), (49) and (40), yields

$$0 = (\Delta x_{1Pf} - \Delta x_{1Ef})(\Delta x_{2Pf} - \Delta x_{2Ef}) + (\Delta x_{3Pf} - \Delta x_{3Ef})(\Delta x_{4Pf} - \Delta x_{1Pf} - \Delta x_{4Ef} + \Delta x_{1Ef}) \tag{51}$$

As before, the stopping condition occurs at the point of closest approach which is found by differentiating the range squared expression, Eq (20), and equating the result to zero at the final time. Again, the result is identically equal to Eq (51). Thus, as before, the stopping condition yields no additional information.

Thus, the linear, normalized, free-time two point boundary value problem consists of the state equations, Eqs (39) and (40), the costate equations, Eqs (43) and (44), the payoff, Eq (41), the Hamiltonian, Eq (42), the optimum control angles, Eqs (46) and (47), the transversality conditions, Eqs (48), (49), and (50), plus the initial values of the states.

Linear Fixed-time TPBVP

The fixed-time problem will be identical to the free-time formulation just shown, with the following exceptions.

1. The value of the Hamiltonian will remain equal to some unknown constant, not necessarily zero. That is, $H(\tau) = K$.

2. The stopping condition will occur simply when the final time is reached. This time will not necessarily correspond to the point of closest approach.

It is important to note that in either linear formulation, the evader's final costates are simply the negative of the pursuer's final costates as shown by the transversality conditions, Eqs (48) and (49). This, coupled with the fact that the costate differential equations are identical for both the pursuer and evader yield the result that the values of the evader's costates are always simply the negative of the pursuer's. That is, $\Delta\lambda_{iP} = -\Delta\lambda_{iE}$. This, in turn, precipitates the additional result that the control angle is identical for each vehicle since the expressions in Eqs (46) and (47) become identical.

Linear Relative Difference TPBVP

Because the evader and pursuer have identical state and costate equations, and because in the linear formulation the optimum control angles are identical for each vehicle ($\alpha_P = \alpha_E$), it is possible to formulate the TPBVP in a set of relative difference equations. Define a set of new state variables $Y_i = \Delta x_{iP} - \Delta x_{iE}$ ($i = 1 \ldots 4$). The system of state equations now reduces to four instead of the original eight. Making use of Eqs (39) and (40),

$$\begin{aligned} Y_1' &= \Delta x_{1P}' - \Delta x_{1E}' \\ &= \Delta x_{2P} - \Delta x_{2E} \\ &= Y_2 \end{aligned} \tag{52a}$$

Likewise

$$Y_2' = 2Y_4 + Y_1 + \Delta u \sin \alpha \tag{52b}$$

$$Y_3' = Y_4 - Y_1 \tag{52c}$$

$$Y_4' = - Y_2 + \Delta u \cos \alpha \tag{52d}$$

where now $\Delta u = u_P - u_E$. This term accounts for the difference between the vehicles' masses and thrusts.

Letting P signify the costates in this formulation, the Hamiltonian now becomes

$$H = P_1 Y_2 + P_2(2Y_4 + Y_1 + \Delta u \sin\alpha) + P_3(Y_4 - Y_1)$$

$$+ P_4(-Y_2 + \Delta u \cos\alpha) \qquad (53)$$

From this, the costate differential equations become

$$P_1' = - P_2 + P_3 \qquad (54a)$$

$$P_2' = - P_1 + P_4 \qquad (54b)$$

$$P_3' = 0 \qquad (54c)$$

$$P_4' = - 2P_2 - P_3 \qquad (54d)$$

The value of this optimum thrust angle, α, can be found by nforcing the necessary and sufficient conditions for either the pursuer or evader.

$$\left.\frac{\partial H}{\partial \alpha}\right|_p = P_2 u_p \cos\alpha - P_4 u_p \sin\alpha$$

$$= 0$$

and

$$\left.\frac{\partial^2 H}{\partial \alpha^2}\right|_p > 0$$

or

$$\left.\frac{\partial H}{\partial \alpha}\right|_E = - P_2 u_E \cos \alpha + P_4 u_E \sin \alpha$$

$$= 0$$

and

$$\left.\frac{\partial^2 H}{\partial \alpha^2}\right|_E < 0$$

The resulting expressions are

$$\sin \alpha = \frac{- P_2}{\sqrt{P_2^2 + P_4^2}} \tag{55a}$$

$$\cos \alpha = \frac{- P_4}{\sqrt{P_2^2 + P_4^2}} \tag{55b}$$

The payoff in relative difference coordinates becomes

$$J = v_1^2 + Y_3^2 \tag{56}$$

Again, the initial values of the state would be known, but the value at the end condition would be unknown. Thus, the transversality conditions yield the following values for the costates at the final condition.

$$P_{1f} = 2Y_{1f} \tag{57a}$$

$$P_{2f} = 0 \tag{57b}$$

$$P_{3f} = 2Y_{3f} \tag{57c}$$

$$P_{4f} = 0 \tag{57d}$$

Note that the costate differential equations, Eqs (54), are completely linear. Those differential equations, with the aid of the boundary conditions, Eqs (57), can be completely solved in closed form. A detailed solution is presented in Appendix A. The final closed for costate expressions are presented below as a function of the characteristic time, τ, and the time at the terminal point, τ_f.

$$P_1 = 4Y_{1f} - 6Y_{3f}(\tau_f - \tau) + 4Y_{3f} \sin(\tau_f - \tau) - 2Y_{1f} \cos(\tau_f - \tau) \tag{58a}$$

$$P_2 = -4Y_{3f} + 4Y_{3f} \cos(\tau_f - \tau) + 2Y_{1f} \sin(\tau_f - \tau) \tag{58b}$$

$$P_3 = 2Y_{3f} \tag{58c}$$

$$P_4 = 4Y_{1f} - 6Y_{3f}(\tau_f - \tau) - 4Y_{1f} \cos(\tau_f - \tau) + 8Y_{3f} \sin(\tau_f - \tau) \tag{58d}$$

Note that to this point in this formulation, nothing has been mentioned concerning stopping conditions since the formulation has been independent of what stopping condition is

used. The final time, τ_f, may be given (fixed-time problem) or may have to be determined by finding the point of closest approach (free-time problem). The free-time stopping condition in relative difference coordinates may be obtained from the original linear stopping condition, Eq (51). Transforming coordinates yields

$$0 = Y_{1f}Y_{2f} + Y_{3f}\,(Y_{4f} - Y_{1f}) \tag{59}$$

Again, note that this is the same result one gets by evaluating the right hand side of the Hamiltonian, Eq (53), at the final time.

IV. Validity of Linear Approximations

Since the linearized equations are actually approximations that assume the encounter occurs somewhere near a set of reference conditions, in this case r_0 and V_0, the equations will be less valid the further from these reference conditions that the operation takes place. That is, errors due to the linearization will occur whenever the spacecrafts' altitudes are different from r_0 and whenever their velocities are different from V_0. It is desirable to have some idea of the errors that are involved. In particular, it should be determined which parameter, spacecraft altitude or velocity, is more critical in inducing these errors.

Comparison Technique

To investigate this, a linear trajectory was compared to several non-linear trajectories. Since the costates, and hence also the control, are functions of the end states, it becomes a relatively simple matter to generate optimum trajectories by starting at some set of final states and integrating backward in time.

The linear trajectory is independent of the specific values of the spacecrafts' altitude or velocity since the linear equations (in relative difference coordinates) deal only with the relative differences between the pursuer's and evader's states. The non-linear equations do however depend upon the exact values of the spacecrafts' positions and

velocities. Thus, it was possible to compare one linear trajectory with several non-linear trajectories by simply insuring that the initial differences (at the final time for backward integration) in positions and velocities were the same in each non-linear run. This allows a determination of the validity of the linear approximations in various actual non-linear situations.

Standard End Conditions

In all open loop computer runs the vehicles were assumed to end at the point of closest approach separated by only a vertical distance (pursuer above the evader). This corresponds to both Y_{2f} and Y_{3f} in Eq (59) equalling zero. That is, the differences between the two spacecrafts' radial velocities and angular positions were zero. The complete set of specific values at the terminal surface were:

$$Y_{1f} = 0.006$$

$$Y_{2f} = 0$$

$$Y_{3f} = 0$$

$$Y_{4f} = 0.0252$$

These values correspond to a terminal situation whereby the point of closest approach occurs when the pursuer is roughly 20 nautical miles above the evader and has a transverse velocity of some 650 feet per second greater than the evader. The author does not wish to imply that there is

anything particularly significant about this choice of parameters. It simply is a reasonable terminal surface. Any set of well behaved values could have been used. Indeed, the author invites the reader to pursue this subject with another such set.

Non-linear Cases

For the non-linear runs, this author chose to specify the evader's exact final position and velocity with the pursuer's being determined by the differences given above; i.e., approximately 20 NM higher and 650 fps faster.

Six non-linear runs were made as shown in Table I. The first of these selected the evader's final orbit to be exactly that orbit used as a reference; i.e., a circular orbit at the earth's surface. This case (Run 1) was to be considered the "best" non-linear situation for the linear approximations.

The next case (Run 2) raised the evader's final altitude by 200 NM, to 3644 NM, but left its final velocity equal to that of the reference orbit (4.269 NM/sec). This means that at the final time, the evader was arriving at the perigee of its orbit. This altitude increase corresponds to a 5.8% increase above the reference orbit.

The remaining cases dealt with changing the terminal velocity of the evader. Runs 3 and 4 decreased the evader's terminal velocity by 5.8% of the reference orbit's velocity. Run 3 assumed the evader ended at the reference altitude

Table I

Evader Non-linear End Conditions

Run	Altitude NM		Transverse Velocity NM/second		
	3444 (Ref)	3644	4.021	4.269 (Ref)	4.517
1	X			X	
2		X		X	
3	X		X		
4		X	X		
5	X				X
6		X			X

(3444 NM) while Run 4 assumed it ended at the higher altitude (3644 NM).

Runs 5 and 6 increased the evader's terminal velocity by the same 5.8% of the reference orbit's velocity. Run 5 ended at 3444 NM, while Run 6 ended at 3644 NM altitude. Appendix B contains the actual trajectories generated by these six non-linear runs. Also presented in Appendix B are the plots of separation distance as a function of time for each of the six runs.

Results

Figures 4 through 7 show relative differences (unitless Y coordinates) of these six runs as a function of time. Also shown on each figure is the curve obtained from the

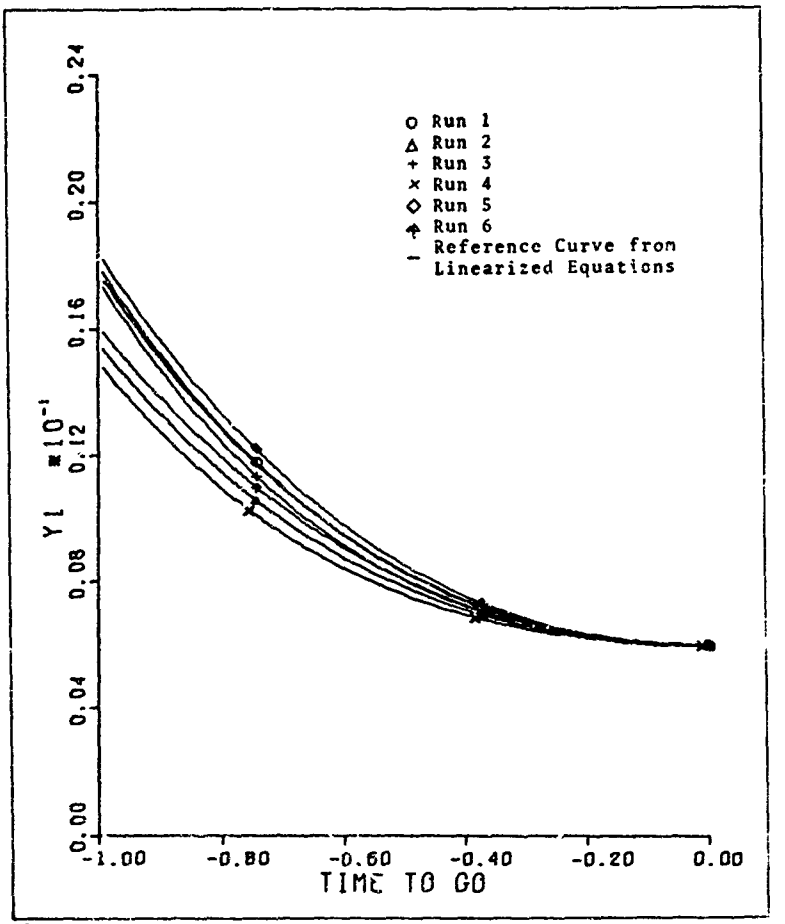

Fig. 4. Comparison of Six Non-linear Optimum Trajectories to the Linear Optimum Trajectory in the Y_1 Relative Difference Coordinates.

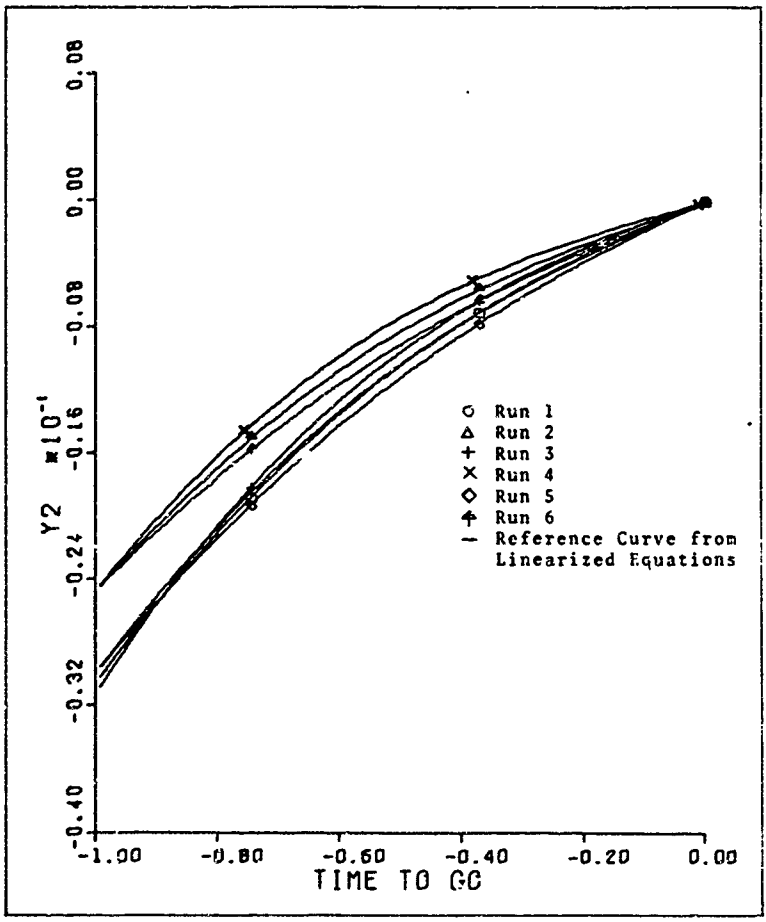

Fig. 5. Comparison of Six Non-linear Optimum Trajectories to the Linear Optimum Trajectory in the Y_2 Relative Difference Coordinate.

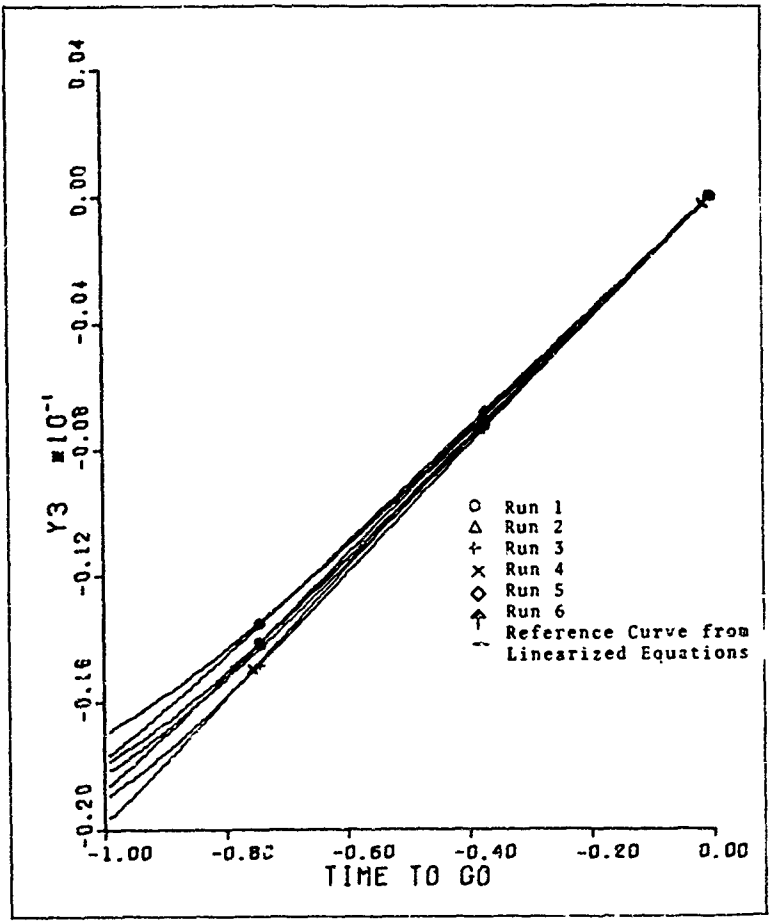

Fig. 6. Comparison of Six Non-linear Optimum Trajectories to the Linear Optimum Trajectory in the Y_3 Relative Difference Coordinate.

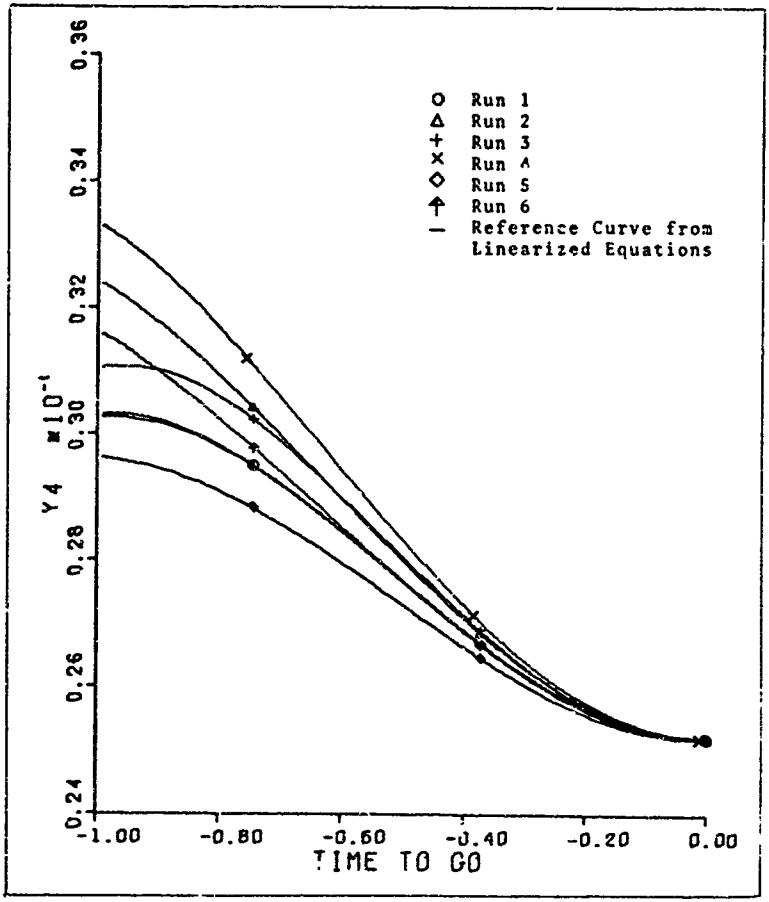

Fig. 7. Comparison of Six Non-linear Optimum Trajectories to the Linear Optimum Trajectory in the Y_4 Relative Difference Coordinate.

linearized equations, although that curve is often indistinguishable from Run 1 (best case).

The time to go in the Y trajectory figures is the characteristic time difference $\tau_f - \tau$. Thus, a time to go of -1.00 corresponds to about 806 seconds before the final time.

Note that in all cases except Y_3 (which relates the vehicles' angular position), the runs eventually tend towards groups based upon like altitude. Thus, Runs 1, 3 and 5 tend as a group to separate from the group composed of Runs 2, 4 and 6. Within each of the groups, the different velocities show their effect.

The exception is in Y_3, Figure 6, where velocity appears to be the key element. Here, the six runs are clustered in pairs, each pair representing one velocity. The different altitudes are hardly noticeable in each pair. In fact, although more noticeable, even the different velocities present only minor errors from the linear case. Indeed, it will be shown later that nearly all fixed-time TPBVP solutions provide excellent agreement in the Y_3 parameter.

In all cases, the velocity increase has an opposite (but like magnitude) effect from a velocity decrease. It also can be seen that a velocity decrease (Run 3) from the reference velocity causes the Y parameters to be offset from the linear, or Run 1, cases in the same direction as the altitude increase, Run 2. Thus the greatest errors in the Y states are caused by the combination of both a velocity

decrease and altitude increase, Run 4.

On the other hand, an altitude greater than the reference orbit (which all real world orbits must be) induces Y state errors which tend to be offset by a vehicle transverse velocity greater than the reference velocity. The amount of velocity increase needed to eliminate the altitude induced error varies for each Y state. For instance, for time within about 0.75 characteristic units of τ_f, Y_4 requires only about a one to one percentage difference. Thus for Y_4, Run 6 which has a 5.8% altitude increase and a 5.8% velocity increase provides an excellent correspondence to the linear and base (Run 1) cases. Y_2, as the opposite extreme, would require considerable more velocity increase, particularly as time becomes further from τ_f. As time becomes close to τ_f, all errors become quite small.

Conclusions

Thus, one sees that the linearized equations are excellent approximations to all the six runs at times very close to the final time. Also, the linearized equations are an excellent approximation to the non-linear situation at the reference orbit (Run 1). Since, for the most part, errors from increased altitude tend to be offset by increased velocity, the linearized equations would tend to be most accurate near the perigees of higher altitude elliptical orbits rather than near their apogees. The accuracy would also decrease for higher altitude circular orbits. The

amount of eccentricity in the elliptical orbit to completely eliminate the increased altitude induced errors would vary for each Y state and would also vary as a function of the time to go.

V. Solutions to the TPBVP's

Fixed-time TPBVP

Chapter IV presented six numerical non-linear trajectories and compared then with respect to the terminal states, against the linear trajectory. Thos trajectories were obtained by backward integration of the equations of motion. This chapter will present the linear solutions to the fixed-time TPBVP's obtained by using as initial conditions selected points from each of the six trajectories discussed in Chapter IV. The linear solutions developed use the analytical formulation of the fixed-time TPBVP for relative difference coordinates that was presente in Chapter III.

Having the backward generated, optimum, non-linear solutions for six runs, it was desired to see how closely the linearized solutions to the TPBVP would approximate these six cases. Thus, three points were chosen from each non-linear run. The points selected were at approximately 0.25, 0.5 and 1.0 characteristic time units from the terminal surface. The set of values of the relative difference states at each of these points was used as initial conditions and input to the fixed-time TPBVP solver. The program iterated on a set of assumed end conditions until it converged to the initial conditions. The linear solutions generated from each of these points is displayed in Figs. 8 through 13.

As would be expected, the errors induced from the linearized solution increase with time. That is, even

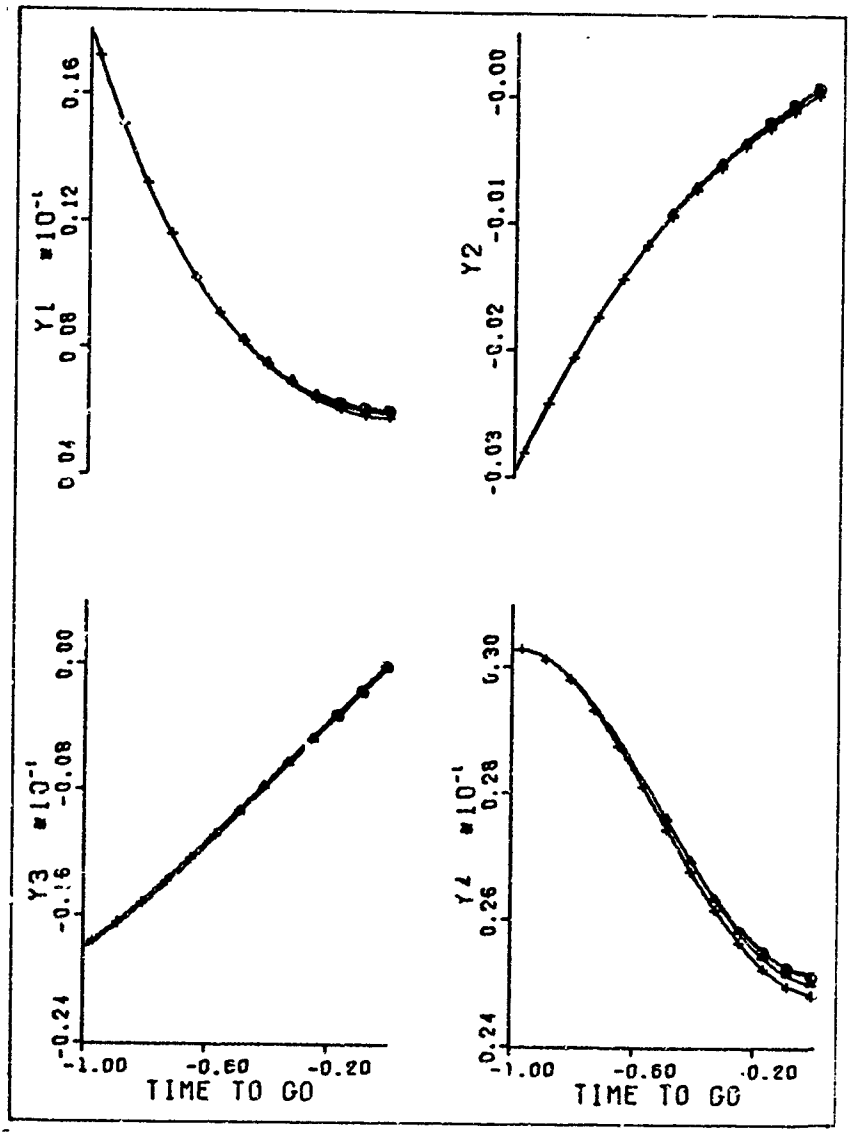

Fig. 8. Trajectories Generated from Solutions to the Fixed-time TPBVP Compared to the Run 1 Non-linear Optimum Trajectory in Relative Difference Coordinates.

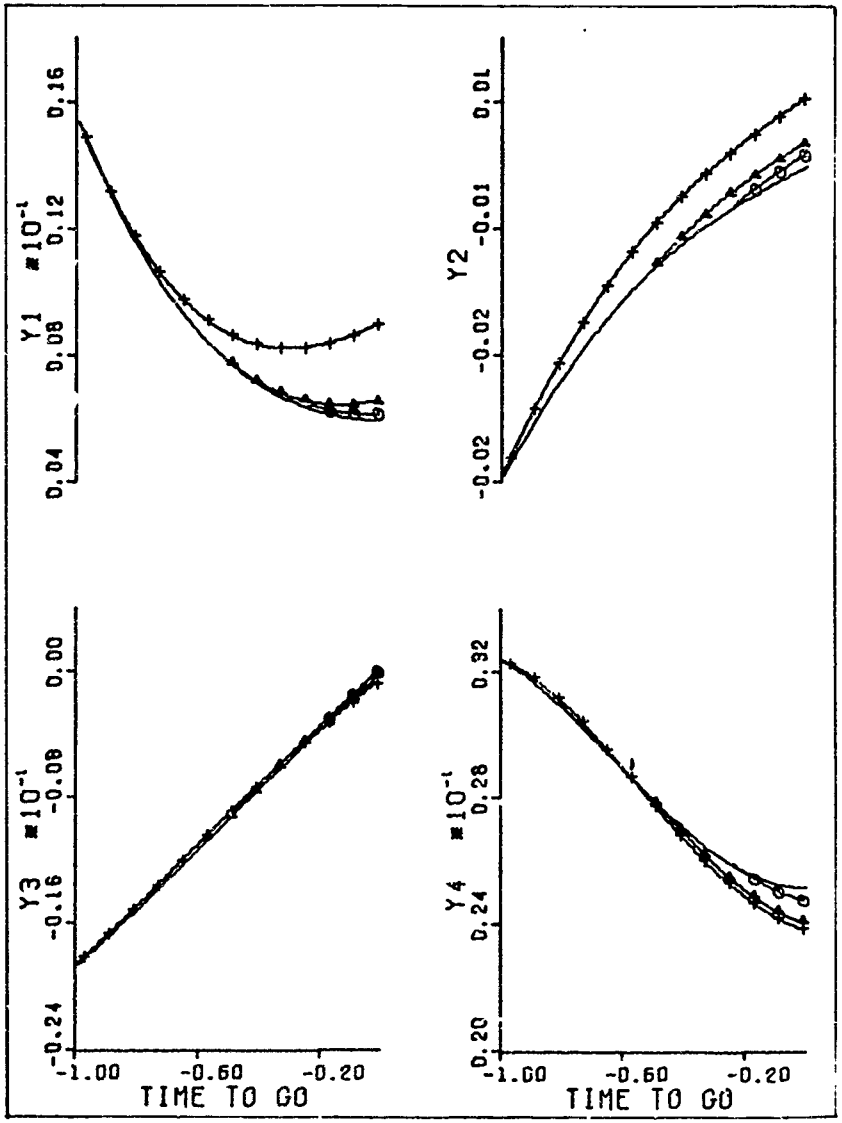

Fig. 9. Trajectories Generated from Solutions to the Fixed-Time TPBVP Compared to the Run 2 Non-linear Optimum Trajectory in Relative Difference Coordinates.

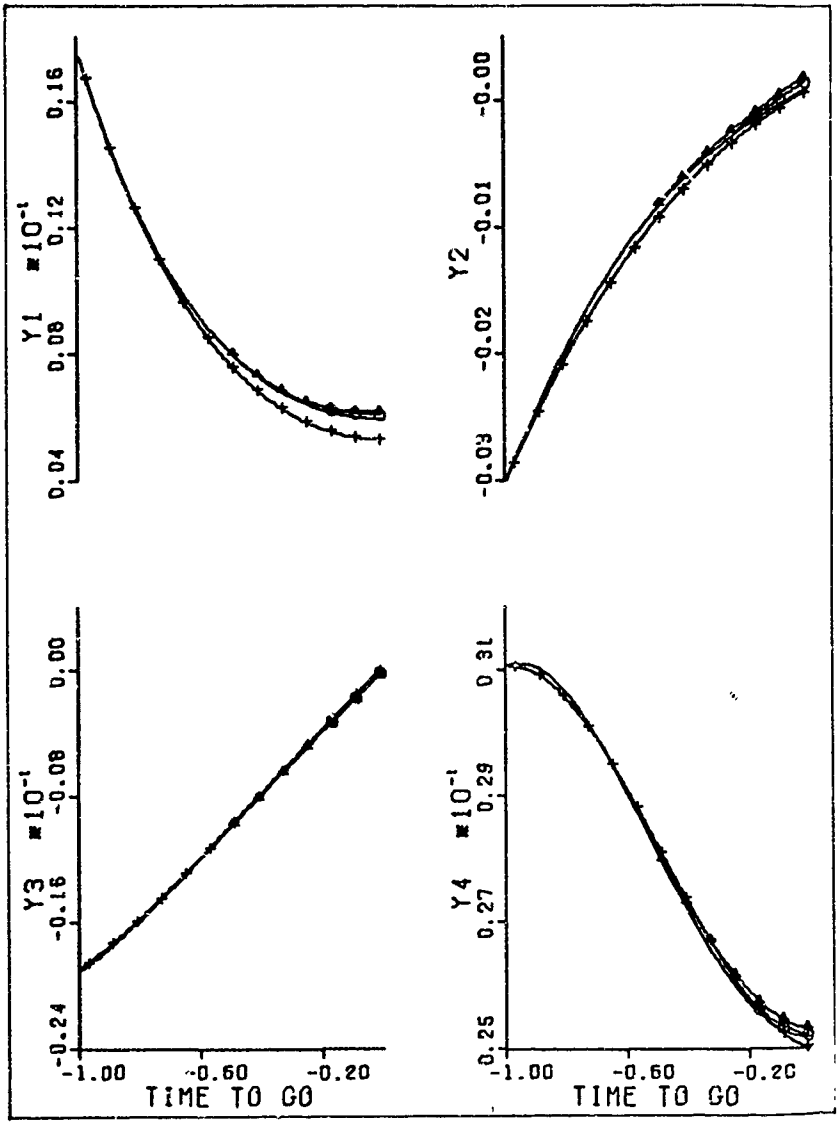

Fig. 16. Trajectories Generated from Solutions to the Fixed-time TPBVP Compared to the Run 3 Non-linear Optimum Trajectory in Relative Difference Coordinates.

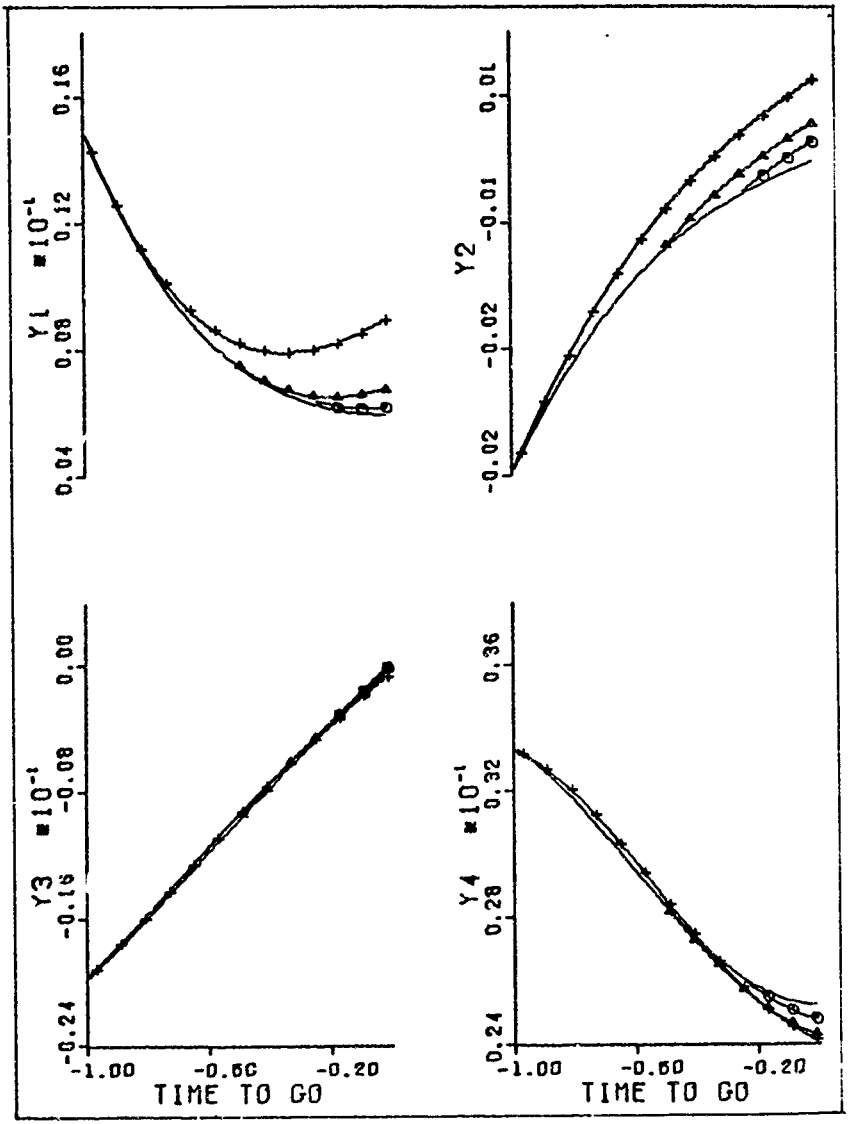

Fig. 11. Trajectories Generated from Solutions to the Fixed-time TPBVP Compared to the Run 4 Non-linear Optimum Trajectory in Relative Difference Coordinates.

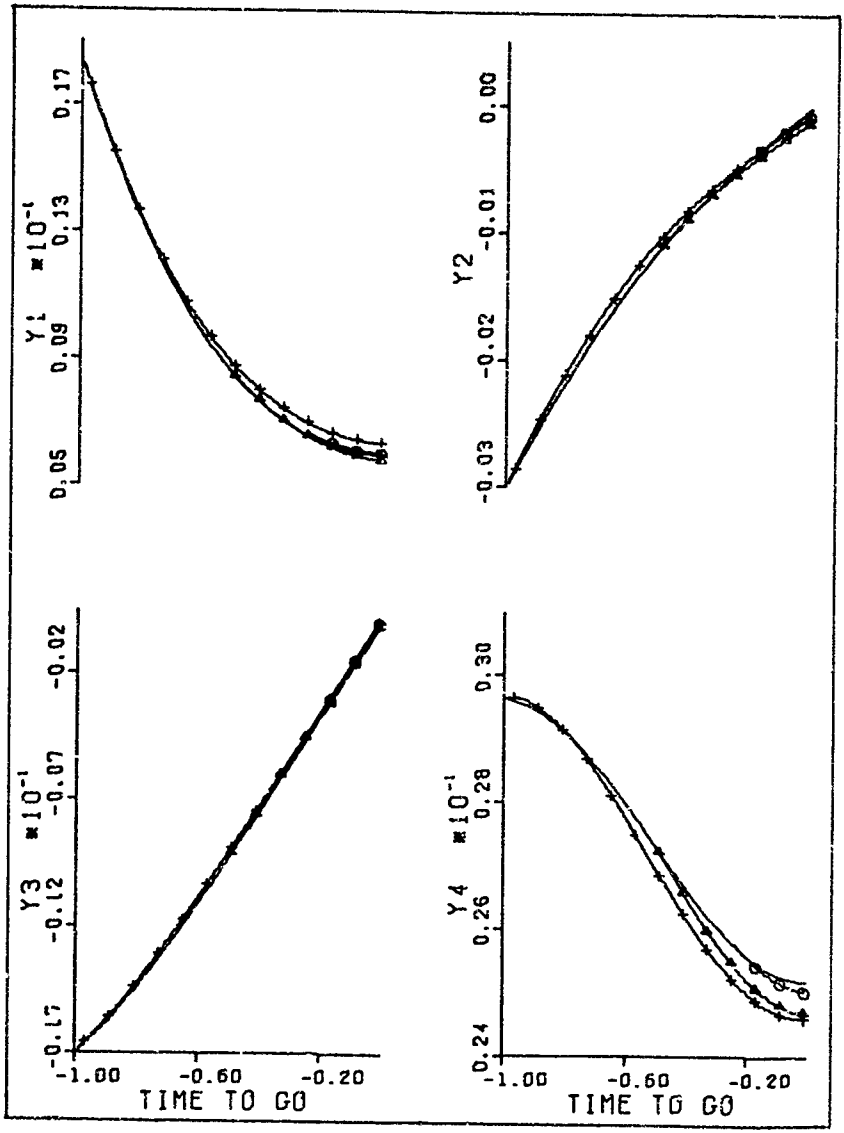

Fig. 12. Trajectories Generated from Solutions to the Fixed-time TPBVP Compared to the Run 5 Non-linear Optimum Trajectory in Relative Difference Coordinates.

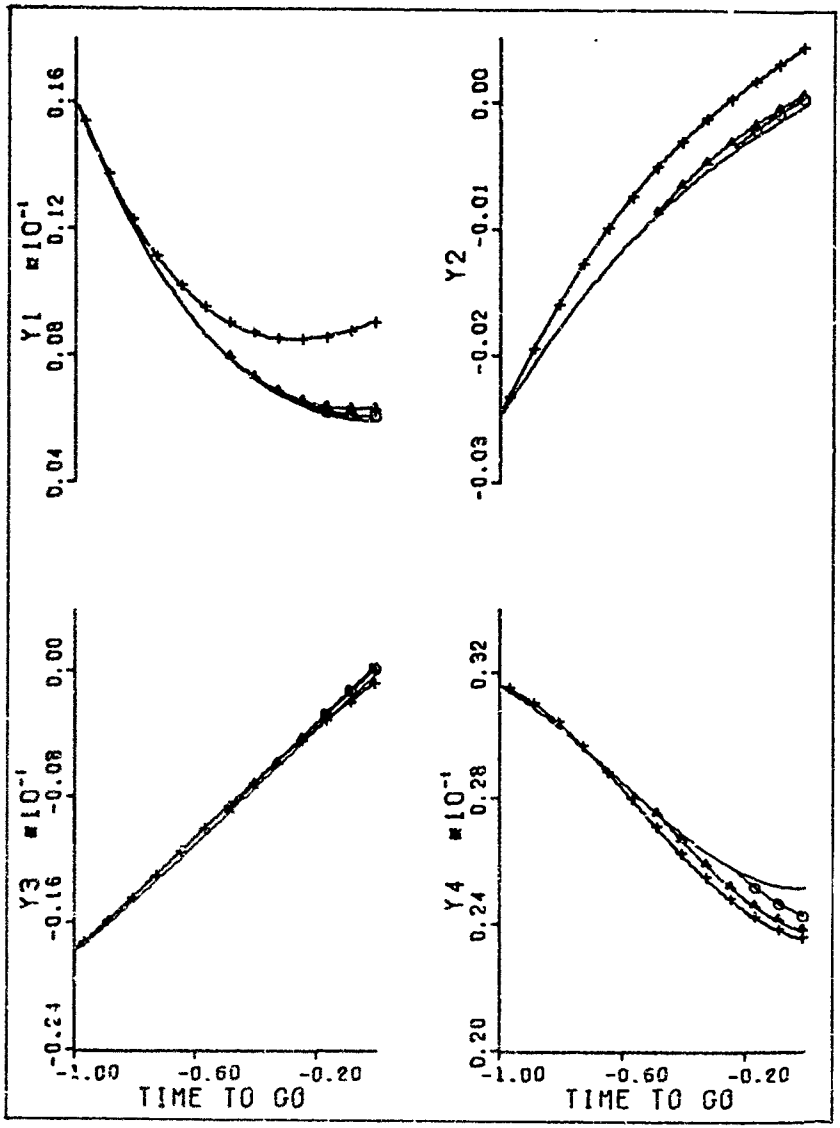

Fig. 13. Trajectories Generated from Solutions to the Fixed-time TPBVP Compared to the Run 6 Non-linear Optimum Trajectory in Relative Difference Coordinates.

tnough the linearized solution starts at the same point as the non-linear solution, the paths tend to diverge with time. Thus for the most part, the closer the input data is to zero time to go the more accurate will be the fixed time solution generated from that point.

Most noticeable is the effect of the different base altitudes (final evader altitude). Runs 1, 3 and 5 assume a final evader altitude of 3444 NM. Runs 2, 4 and 6 assume a final evader altitude of 3644 NM. Three things are readily noticeable. First, each run in each set appears almost identical to the other runs in that set. That is, the results of Run 1 appear almost identical to the results of Run 5. Likewise for the other set, Runs 2, 4 and 6. Secondly, those runs at the higher base altitude (Runs 2, 4 and 6) exhibit substantially greater errors than do those runs at the lower altitude (Runs 1, 3 and 5). Thirdly, the effects of the different base velocities are practically indistinguishable.

Thus, for the fixed-time solutions, the actual base altitude is the most important consideration. At this point it becomes apparent that the further from the linearized reference altitude one gets, the less accurate will be his fixed time solution. Here, there appears to be no such thing as velocity compensation for altitude errors as there was in Chapter IV. Based on the fixed-time results, it appears most important to linearize the equations of motion

about an orbit whose altitude is as close to the actual altitude of operation as possible.

Free-time TPBVP

It was attempted to generate free-time solutions from each of the same points where fixed-time solutions were generated in the previous chapter. The free-time problem did not, of course, specify for what time the input data corresponded. Instead, the free-time solver selected the time by driving the final range squared rate expression to zero (within some limits).

The method used, as discussed before, was actually to solve several fixed time problems, forcing the final range squared rate toward zero by use of a Newton-Raphson technique. To solve a fixed time problem requires an estimate of the final time. It was found that the value of this initial estimate could be rather arbitrary since the program would iterate to within an order of magnitude of the correct value within a very few cycles. However, it was found that the use of a smaller initial estimate of time to go greatly decreased the overall convergence time since the time to perform each cycle or iteration is directly related to the estimate of time to go.

One immediate result of experimentation was that it was extremely difficult to generate free-time solutions for those data inputs close to zero time to go. That is, of the input data from 0.25, 0.5 and 1.0 characteristic time units, only

the data from 1.0 consistently yielded any results. Those results are displayed in Figs. 14 through 19. The shorter time problems (0.5 and particularly 0.25) required either very accurate initial estimates, or very loose convergence tolerances and lengthy convergence (i.e., computer) time. Since it was desired to obtain solutions that did not require extremely accurate initial estimates and since the lengthy time required for solution of the short time to go problems was greater than the time to go, these particular situations were not investigated in great detail. Instead, the conclusion is made that the initial free-time solution must be generated when the time to go is still reasonably large. This initial free-time solution could then be updated and improved upon.

Analysis of the free-time solutions shown in Figs. 14 through 19 yields a conclusion similar to that for the fixed-time solutions. Again, the six runs are divisible into two distinct sets. Each set represents a different final altitude. That is, Runs 1, 3 and 5 all resemble each other and Runs 2, 4 and 6 also resemble each other. Also, as in the previous chapter, the higher altitude runs (Runs 2, 4 and 6) induce greater errors than do the runs at the lower altitude. To yield higher altitude runs with smaller errors would require the convergence tolerances to be made smaller. This, of course, would increase the time for convergence. The convergence time for those cases in this study varied from 15% to 25% of the time to go. Further increases in this

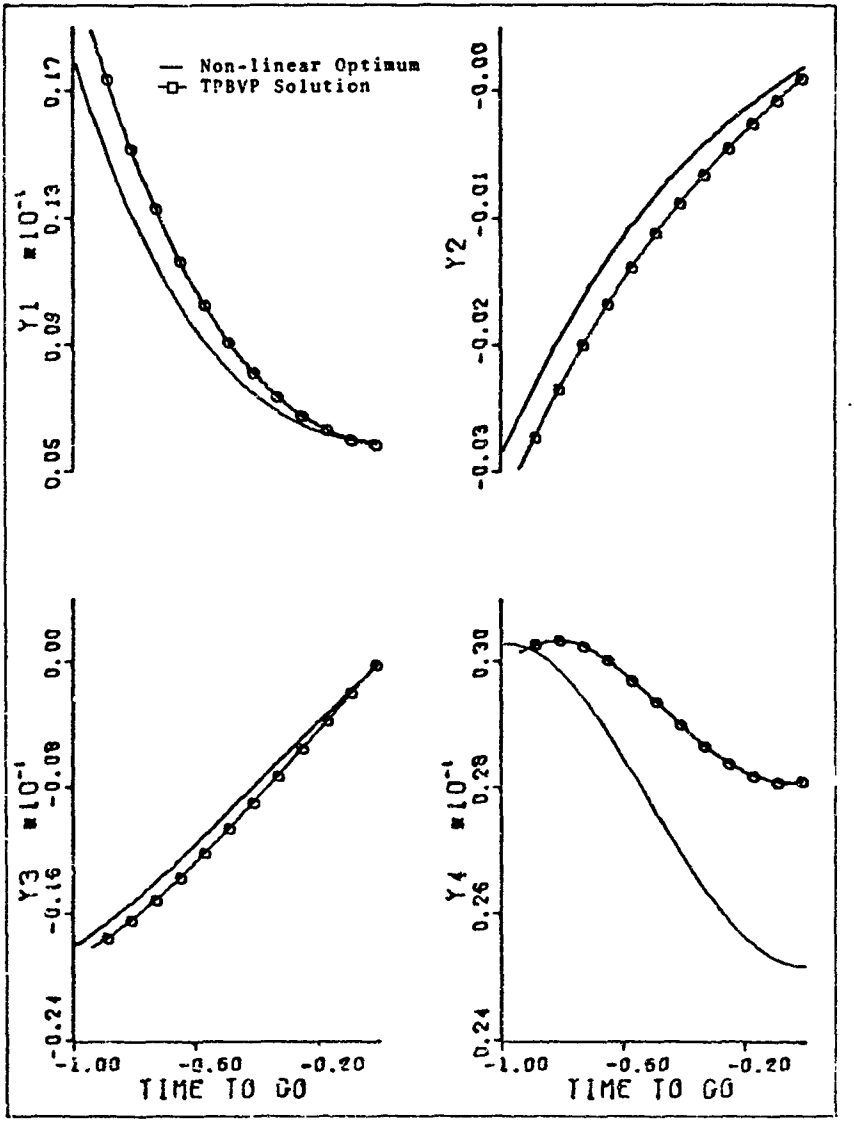

Fig. 14. Trajectory Generated from Solution to the Free-time TPBVP Compared to the Run 1 Non-linear Optimum Trajectory in Relative Difference Coordinates.

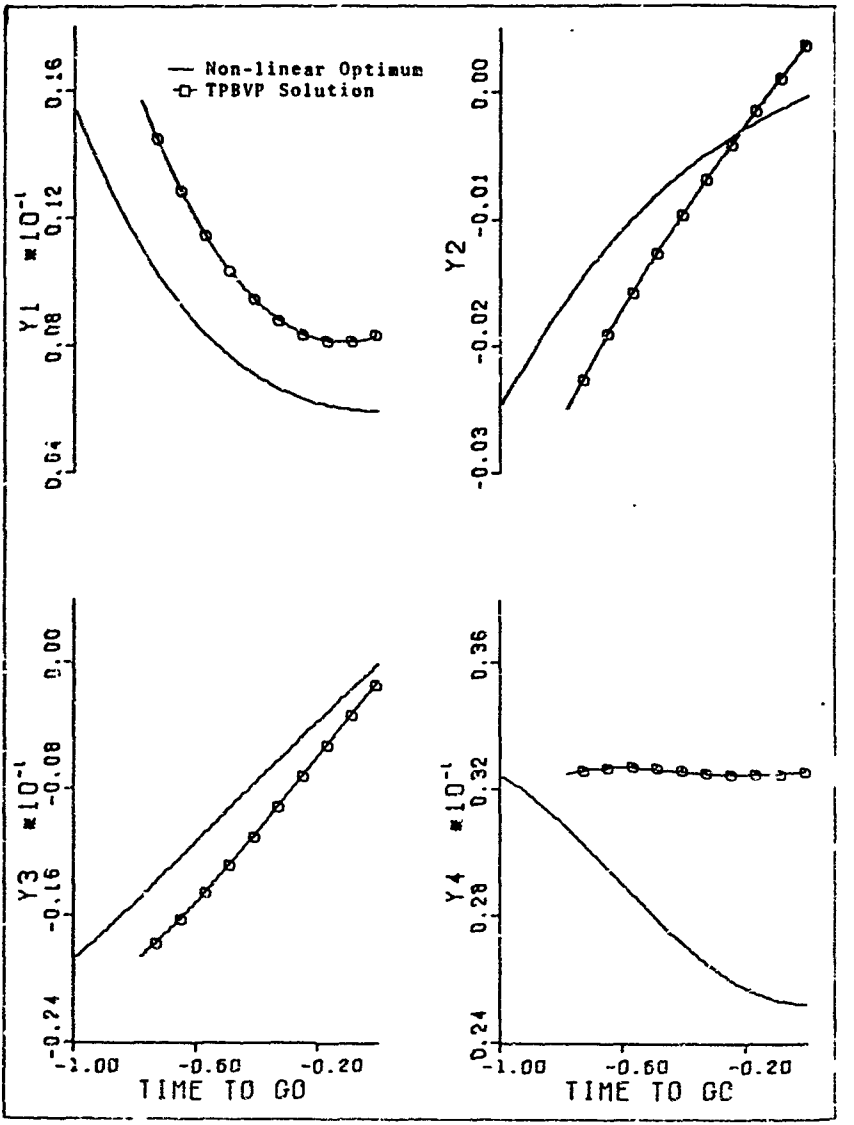

Fig. 15. Trajectory Generated from Solution to the Free-time TPBVP Compared to the Run 2 Non-linear Optimum Trajectory in Relative Difference Coordinates.

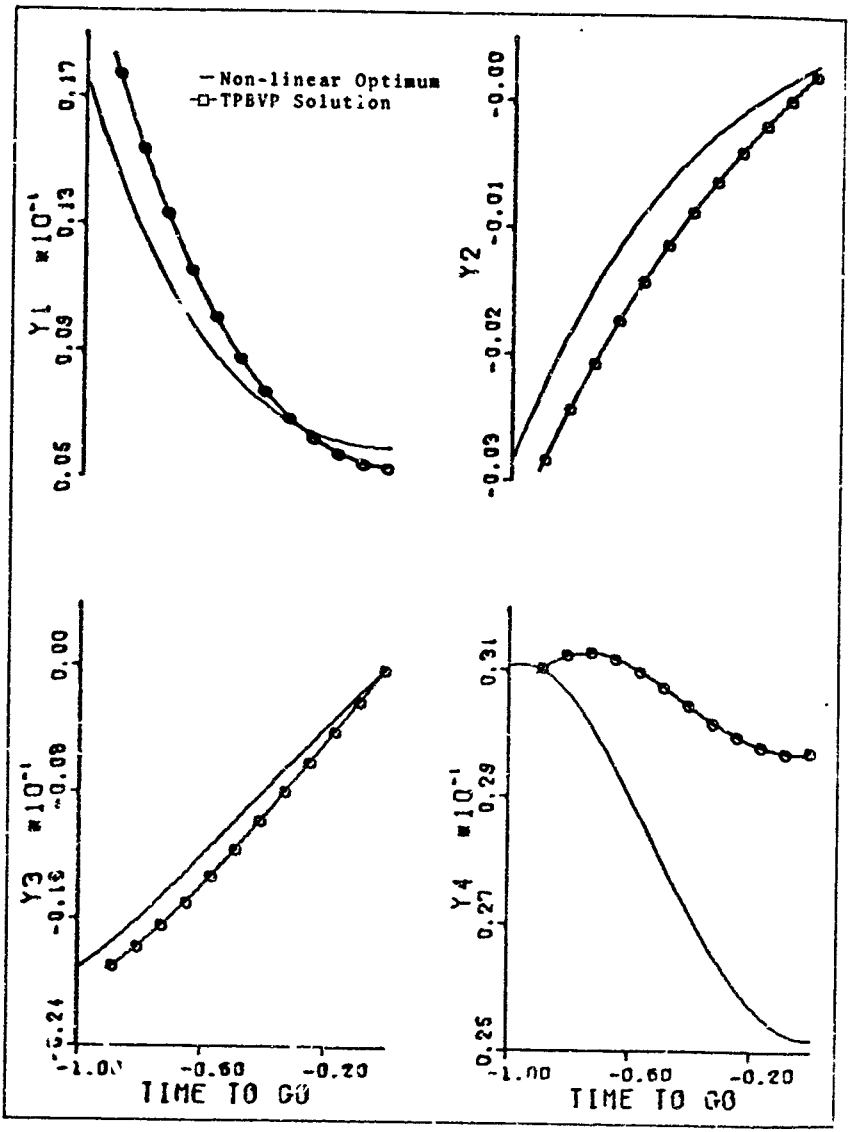

Fig. 16. Trajectory Generated from Solution to the Free-time TPBVP Compared to the Run 3 Non-linear Optimum Trajectory in Relative Difference Coordinates.

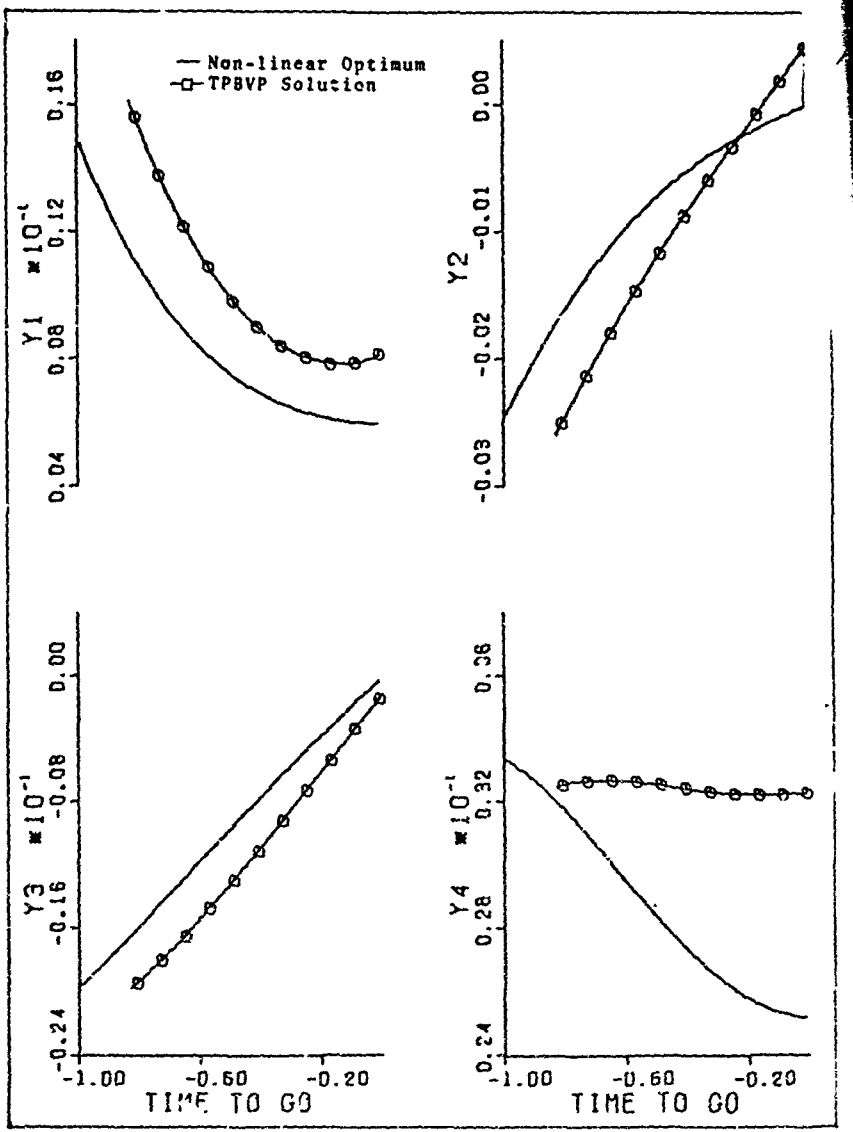

Fig. 17. Trajectory Generated from Solution to the Free-time TPBVP Compared to the Run 4 Non-linear Optimum Trajectory in Relative Difference Coordinates.

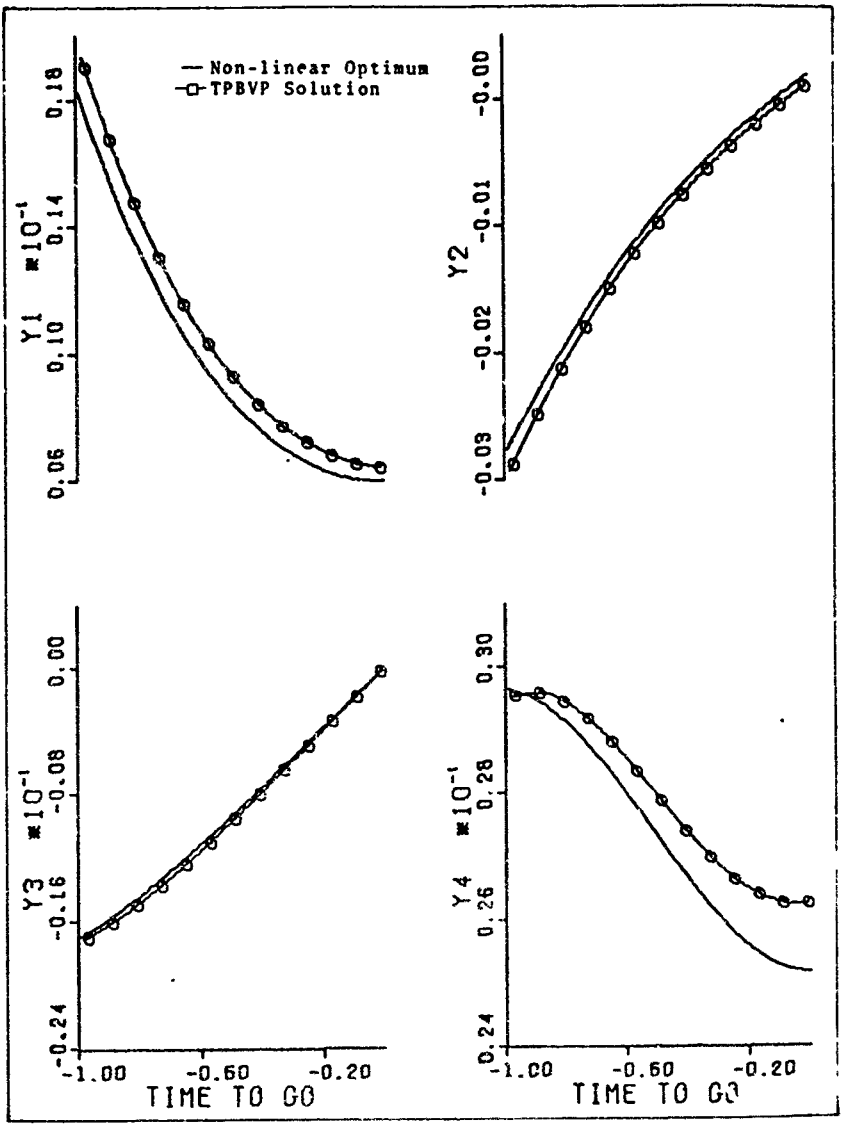

Fig. 18. Trajectory Generated from Solution to the Free-time TPBVP Compared to the Run 5 Non-linear Optimum Trajectory in Relative Difference Coordinates

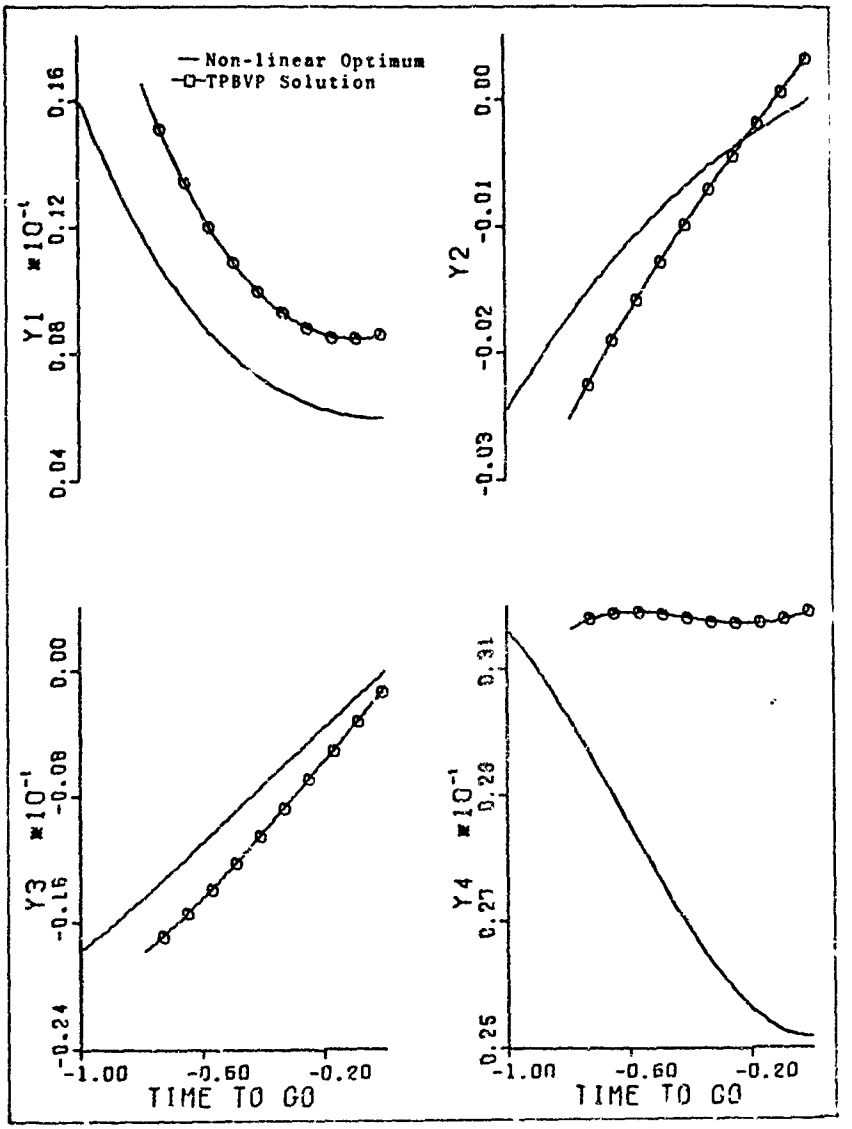

Fig. 19. Trajectory Generated from Solution to the Free-time TPBVP Compared to the Run 6 Non-linear Optimum Trajectory in Relative Difference Coordinates.

convergence time would decrease the worth of the solutions.

Again, the differences induced by the velocity variations are indistinguishable. Thus, the same conclusion is reached. The major sources of error is due to operating at an altitude other than the linear reference orbit. This error may be at least partially diminished by reducing the allowable convergence tolerances, but this increases the required time for convergence.

Some additional computational details are given in Appendix C.

VI. Pseudo Closed Loop Control Law

A closed loop control law would be desirable in any real time encounter. That is, you as a player would like to be able to take advantage of any non-optimal play by your opponent, thus bettering your final payoff over that which would develop had you not taken advantage of your opponent's error.

Normally, closed loop solutions can be generated for linear-quadratic problems. Since the situation treated in this thesis is pseudo linear, linear in state but non-linear in control, it was attempted to develop (or rather approach) a closed loop solution as closely as possible. This chapter discusses the development of that pseudo closed loop control law.

Matrix Formulation

The relative difference state equations, Eqs (52), can be written in the following matrix form:

$$[Y'] = [F][Y] + [G] \tag{60}$$

where

$$[F] = \begin{bmatrix} 0 & 1 & 0 & 0 \\ 1 & 0 & 0 & 2 \\ -1 & 0 & 0 & 1 \\ 0 & -1 & 0 & 0 \end{bmatrix} \tag{61}$$

and

$$[G] = \begin{bmatrix} 0 \\ \Delta u \sin \alpha \\ 0 \\ \Delta u \cos \alpha \end{bmatrix} \qquad (62)$$

From the F matrix, one can find the fundamental or transition matrix, $\Phi(\tau_f,\tau_0)$, for this system of equations. Appendix E contains that Φ derivation.

Having the transition matrix, the end states, Y_f, can be written in terms of the present measurable states Y_0:

$$[Y_f] = [\Phi(\tau_f,\tau_0)][Y_0] + \int_{\tau_0}^{\tau_f} [\Phi(\tau_f,\tau)][G(\tau)]d\tau \qquad (63)$$

where $G(\tau)$ contains the control parameters as a function of characteristic time tau and the end states. Thus if the control matrix were zero, the problem would degenerate into a strictly linear problem and the final states could immediately be found by using the transition matrix to operate on the initial states. In fact, a very rough first approximation of the final states could be made in just that way, i.e., assuming no control. This rough approximation of the final states could then be used to provide the control inputs. This technique would be one of the easiest to implement, however, it would have to be updated at very short time increments due to the erroneous assumption of zero thrust. Also, this would not be a closed loop control.

Development

A theoretically more accurate, although more complex solution can be generated by first solving the free-time TPBVP thus getting initial estimates of Y_f and τ_f. These estimates can then be used in the control angle expressions. Having a control program it can simultaneously be used to numerically integrate the equations of motion forward (assuming both players play optimally) and to fly the actual trajectory. At periodic intervals, direct measurements of the opponent's actual state can be made. These measurements can be compared with the numerically integrated values. The differences can be used to update the control program through the use of the differential of Eq (63). That differential must allow for changes in both the final states and final time. Thus,

$$[\Delta Y_{ff}] = [\Phi(\tau_f,\tau_0)][\Delta Y_0] + \frac{\partial}{\partial \tau_f}\{[\Phi(\tau_f,\tau_0)][Y_0]\}\Delta\tau_f$$

$$+ \frac{\partial}{\partial \tau_f}\{\int_{\tau_0}^{\tau_f}[\Phi(\tau_f,\tau)][G(\tau)]d\tau\}\Delta\tau_f$$

$$+ \frac{\partial}{\partial Y_f}\{\int_{\tau_0}^{\tau_f}[\Phi(\tau_f,\tau)][G(\tau)]d\tau\}[\Delta Y_f] \qquad (64)$$

where ΔY_0 is the difference between the values of the present state as measured and as calculated from the free-time TPBVP, ΔY_{ff} is the amount that must be added to the present estimate of Y_f and $\Delta\tau_f$ is the amount that must be added to the present

estimate of τ_f (which too was determined from the solution to the TPBVP). ΔY_f is the difference between the corrected Y_f at τ_f and the original value of Y_f as is seen in Fig. 20. These parameters are related in the following way:

$$\Delta Y_{ff} = \Delta Y_f + \dot{Y}_f \Delta\tau_f$$

or

$$\Delta Y_f = \Delta Y_{ff} - \dot{Y}_f \Delta\tau_f \tag{65}$$

Equation (65) can be used to replace ΔY_f in Eq (64). The result would be an expression in terms of the initial known quantities (Y_0 and ΔY_0) and the two unknowns ΔY_{ff} and $\Delta\tau_f$. Another equation is needed to facilitate determination of these unknowns. That other equation can be formed from the Hamiltonian which must remain equal to zero at the "new" final time $\tau_f + \Delta\tau_f$. Thus $\Delta H_f = 0$. Expanding,

$$\frac{\partial H}{\partial Y_f} \Delta Y_f + \frac{\partial H}{\partial \tau_f} \Delta\tau_f = 0$$

But since from Eq (59), $\frac{\partial H}{\partial \tau_f} = 0$, the above equation becomes:

$$\frac{\partial H}{\partial Y_f} \Delta Y_f = 0 \tag{66}$$

Substituting Eq (65) into Eq (66) results in the second equation in terms of ΔY_{ff} and $\Delta\tau_f$:

$$\frac{\partial H}{\partial Y_f} (\Delta Y_{ff} - \dot{Y}_f \Delta\tau_f) = 0 \tag{67}$$

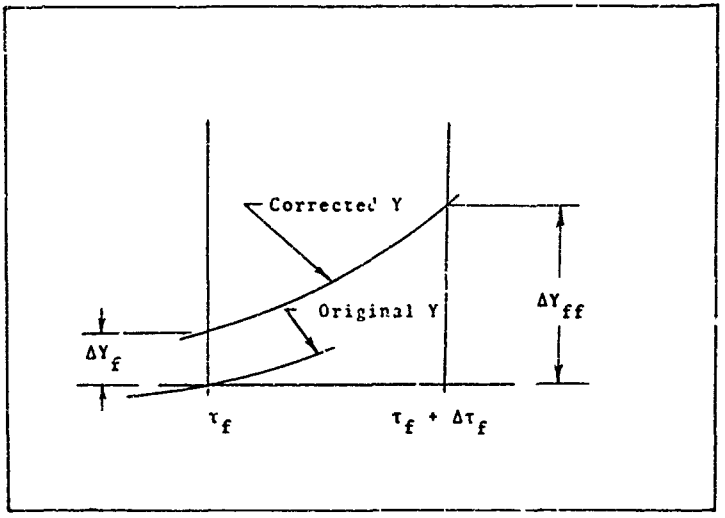

Fig. 20. Relationship Between Differences in Y State at the Original Final Time τ_f and at the Corrected Final Time $\tau_i + \Delta\tau_f$.

Now, the combination of Eqs (64) and (65) can be solved for ΔY_{ff} in terms of $\Delta\tau_f$. Those expressions can then be used in Eq (67) to provide a scalar equation relating $\Delta\tau_f$ to the known initial states. Solving, the value for $\Delta\tau_f$ can then be used to provide ΔY_{ff}, the quantity which must be added to the original Y_f estimate.

These solutions, then, are the corrections that must be applied to the original estimate of the final states and final time. These new estimates can then be used to update the values of the control variables. The updated controls

can then be used until another update is desired. This next update could be required after some finite amount of time had passed or after the errors between the measured and calculated trajectories (ΔY_0), due to the opponent's non-optimal play, exceed some specified tolerance. At that point, Eqs (64), (65) and (67) can then again be solved to provide another control update.

This technique, of using Eqs (64), (65) and (67) to update the control by a function of the present measured state, is the pseudo closed loop control law that this chapter set out to derive.

Numerical Test

This technique was tested numerically against two non-optimum evaders. The basic situation was that of Run 4, described earlier in this report. In the first case, the evader's thrust angle was held constant at 180° and in the second case, it was held constant at a value of 0°. In both cases it was assumed that the exact solution to the TPBVP was known. This of course could not be true in an actual operation, but served as a test case for this analytical investigation. The exact solution yields the final states that would exist if both vehicles had been playing optimally.

For comparison purposes, each non-optimum evader also was "flown" against a pursuer who followed his open loop control. The minimum separation distances for these various trajectories are tabulated in Table II.

Table II

Minimum Separation Distances (NM)

Case	Open Loop	Pseudo Closed Loop
1. Both Optimum	20.6	----------
2. Evader Thrust at 180°	13.4	13.1
3. Evader Thrust at 0°	13.7	44.9

Since in the non-optimum cases it is the evader who is playing non-optimally, the final separation distance should be less than when both vehicles are playing optimally. In addition, the pseudo closed loop technique should further decrease that final separation distance.

Based on these premises, Table II appears to be plagued with a large inconsistency in that the correction technique applied against the 0° thrust angle evader increases the final separation distance over the open loop run!

Although that increase is discouraging, deeper analysis of the resulting numerical test indicates the situation may not be as bad as it appears. That is, the corrections ΔT_f and ΔY_{ff} that were calculated in the course of the test were in the correct direction. The magnitude of the ΔY_{ff} correction, though, were too great too soon. The magnitude of these corrections being too large caused the pursuer to over correct his control program. This over correction resulted in the pursuer being taken off his optimum trajectory. By

the time the control law realized it had over corrected, and started to recompensate, the scenario had reached the terminal surface (the point of closest approach).

It should be noted that the updating by the control system was performed at a set periodic interval of about every hundred seconds. The entire open loop game lasted some 800 seconds while the closed loop game terminated after only 570 seconds. Thus, in the latter case, only five updates were made during the entire game. Since the errors ΔY_0's grow between updates, those errors may have grown so large as to invalidate the linearization. To check that possibility, one additional test was run against the 0° evader with an update interval half as long (i.e., about 50 seconds). The final separation distance from that run was only 34.6 NM, a marked improvement. Thus it is felt that the use of a shorter interval between updates would keep the ΔY_0 errors smaller and thus diminish the over correction of the control. This in turn would improve the final separation distance.

Another possible explanation, more basic in nature, for the increased final separation distance is that the situation investigated in this entire thesis may just not lend itself to this particular quantitative analysis. That is, the assumed low thrusts and large mass (made so to allow the original constant mass assumption) coupled with the rather large value of final relative velocity between the spacecraft may simply not allow any great degree of control.

To justify keeping the masses constant, the thrust of the pursuer had been set at 500 lb. and the weight of the spacecraft had been set at 10,000 lb. The final transverse velocity difference between the spacecraft was set at about 650 feet per second, to insure the two vehicles would "pass" each other. Observing that the vehicles had been thrusting in the third quadrant (with the evader leading the pursuer) for some 800 seconds before the final conditions occur, it can be shown that at the initiation of the encounter the relative closing rate would be 650 fps plus an additional value of up to 1600 fps. Thus, the initial closing velocity between these two spacecraft is in the neighborhood of 1500 fps.

Thus, with an initial closing rate of that high, it appears that the small thrust to weight ratios may simply be too small to have much pronounced effect upon the final separation distance.

Hence, the results of this numerical test of the pseudo closed loop control technique are, unfortunately, inconclusive. However, it is recommended that future effort in this particular area use shorter update intervals and larger thrust to weight ratios, even at the expense of the constant mass assumption.

VII. Conclusions and Recommendations

Conclusions

A two-dimensional pursuit-evasion encounter between two constant thrust spacecraft in near-earth orbit has been formulated at a differential game with control being provided by the thrust angle. The spacecraft were given a high closing velocity to insure the game would go to completion. The thrust to weight ratios were kept low in order to assume constant mass vehicles. The encounter took place in an inverse square gravity field near the earth's surface.

The non-linear equations of motion were linearized about a circular reference orbit at the earth's surface. Open loop solutions were generated for both sets of equations backward in time from selected terminal states. The linear open loop solution compared quite favorably with the non-linear solutions for both vehicles playing optimally. Operation at altitudes above the reference orbit induced errors, but these were partially offset by allowing the velocities to be greater than the reference orbit.

The linearization of the equations of motion provided for closed form solutions to the costate vector. This, in turn, allowed the control (thrust angle) expressions to be simplified.

Using the simplified, or approximate, control expressions, both the fixed-time and free-time two point boundary value problems were solved. As was expected, the errors in

these linearized solutions diverge from the actual trajectory as time passes. In addition, off reference altitudes were again found to be the greatest contributor of errors, only now the errors did not seem to be decreased appreciably by any compensating velocity errors.

It was found that fairly accurate free-time solutions could be generated (within acceptable computer time limits also) by requiring only moderate convergence accuracies.

As the terminal surface was approached, it became increasingly more difficult to obtain a free-time solution. Thus, in an actual encounter, the initial free-time solution should be generated when the time to go is still reasonably large. This initial free-time solution could then be updated and improved.

A pseudo closed loop control technique was developed based upon the fundamental or transition matrix of the linearized equations of motion. However, its effects upon the particular encounter tested were inconclusive, probably due to the inherent sensitivities of the problem. That is, the assumed low thrust to weight ratios coupled with the high closing velocities appear to diminish the effectiveness of the control.

Recommendations

Investigation of this problem has led this author to three main recommendations for further study.

First, since altitude is the greatest contributor to errors in the linearized solutions, it would be fruitful to

linearize the equations of motion about an orbit which more nearly approximates the altitude of operation. Once that is done, then the results can be compared with the non-linear solutions. This should improve the overall accuracies.

Second, attempt to test a control program based strictly upon the transition matrix. Thus, the present measured states could very quickly be transformed to end states, and the exact transformation selected would be the one which gave the correct terminal surface, i.e., minimum separation distance. This method would be inherently erroneous as the application of the transition matrix requires the assumption that no control is to be provided. However, since the process would be so rapid, it could easily be updated (repeated) almost instantaneously and might allow for a very easy control system. The purpose of the test would be to check the accuracy of the technique.

Lastly, since this author encountered apparent sensitivity problems with this low thrust to weight, high closing velocity scenario, it is recommended that future investigators assume larger thrust to weight ratios, even at the expense of the constant mass assumption.

Bibliography

1. Anderson, G. M. Lecture Notes: "Trajectory Optimization Techniques," Wrignt-Patterson AFB, Ohio, Air Force Institute of Technology, 1970.

2. Billik, B. H. "Some Optimal Low-Acceleration Rendezvous Maneuvers." AIAA Journal, 2: 510-516 (March 1964).

3. Bryson, A. E. and Y. Ho. Applied Optimal Control. Waltham, Massachusetts: Blaisdell Company, 1969.

4. Wong, R. E. "Some Aerospace Differential Games." Journal of Spacecraft, 4: 1460-1464 (November 1967).

Appendix A

Closed Form Costate Solution

The linear relative difference costate differential equations, Eqs (54), can be solved in closed form, with the aid of the costate end conditions, Eqs (57), to yield expressions for the costate vector. The differential equations are repeated below:

$$P_1' = -P_2 + P_3 \tag{54a}$$

$$P_2' = -P_1 + P_4 \tag{54b}$$

$$P_3' = 0 \tag{54c}$$

$$P_4' = -2P_2 - P_3 \tag{54d}$$

The end conditions have been given as:

$$P_{1f} = 2Y_{1f} \tag{57a}$$

$$P_{2f} = 0 \tag{57b}$$

$$P_{3f} = 2Y_{3f} \tag{57c}$$

$$P_{4f} = 0 \tag{57d}$$

It can readily be seen that P_3 is a constant.

$$P_3(\tau) = 2Y_{3f} \qquad \text{(A-1)}$$

Using Cramer's rule on the remaining three equations and letting D indicate differentiation with respect to τ yields:

$$\begin{vmatrix} D & 1 & 0 \\ 1 & D & -1 \\ 0 & 2 & D \end{vmatrix} P_1 = \begin{vmatrix} P_3 & 1 & 0 \\ 0 & D & -1 \\ -P_3 & 2 & D \end{vmatrix}$$

or

$$(D^3 + D)P_1 = 3P_3 \qquad \text{(A-2)}$$

The roots of the characteristic equation of the system are 0, $\pm$ i. The complementary solution is therefore

$$C_1 + C_2 \sin \tau + C_3 \cos \tau$$

Now, the forcing function is simply a constant. Since there is already a constant term in the complementary function, one must assume a particular integral of the form $\underline{P} = K\tau$. Putting this assumed solution into the differential equation Eq (A-2) gives

$$0 + K = 3P_3$$

Thus,

$$P_1 = C_1 + 3P_3\tau + C_2 \sin \tau + C_3 \cos \tau \qquad \text{(A-3)}$$

Likewise,

$$(D^3 + D)P_2 = 0$$

which yields

$$P_2 = C_4 + C_5 \sin \tau + C_6 \cos \tau \qquad \text{(A-4)}$$

and

$$(D^3 + D)P_4 = \begin{vmatrix} D & 1 & P_3 \\ 1 & D & 0 \\ 0 & 2 & -P_3 \end{vmatrix}$$

$$= 2P_3 + P_3$$

$$= 3P_3$$

Again, one must test a particular integral of the form $\underline{P} = K\tau$ and find that $K = 3P_3$. Thus,

$$P_4 = C_7 + 3P_3\tau + C_8 \sin \tau + C_9 \cos \tau \qquad \text{(A-5)}$$

These three equations for P_1, P_2 and P_4 may now be substituted into the original costate differential equations to obtain relationships among the nine constants $C_1, C_2, \ldots C_9$. Differentiating Eq (A-2)

$$P_1' = 3P_3 + C_2 \cos \tau - C_3 \sin \tau \qquad \text{(A-6)}$$

but

$$P_1' = -P_2 + P_3$$

$$= -C_4 - C_5 \sin \tau - C_6 \cos \tau + P_3 \qquad \text{(A-7)}$$

Equating like terms in Eqs (A-6) and (A-7),

$$C_4 = -2P_3$$

$$C_6 = -C_2$$

$$C_5 = C_3$$

Now differentiating Eq (A-4)

$$P_2' = C_5 \cos \tau - C_6 \sin \tau$$

$$= C_3 \cos \tau + C_2 \sin \tau \qquad \text{(A-8)}$$

but

$$P_2' = -P_1 + P_4$$

$$= -C_1 - 3P_3\tau - C_2 \sin \tau - C_3 \cos \tau$$

$$+ C_7 + 3P_3\tau + C_8 \sin \tau + C_9 \cos \tau \qquad \text{(A-9)}$$

Equating like terms in Eqs (A-8) and (A-9) yields

$$C_7 = C_1$$

$$C_8 = 2C_2$$

$$C_9 = 2C_3$$

It is now possible to write the costate equations in terms of only three unknown constants:

$$P_1 = C_1 + 3P_3\tau + C_2 \sin\tau + C_3 \cos\tau \qquad \text{(A-10)}$$

$$P_2 = -2P_3 - C_2 \cos\tau + C_3 \sin\tau \qquad \text{(A-11)}$$

$$P_4 = C_1 + 3P_3\tau + 2C_2 \sin\tau + 2C_3 \cos\tau \qquad \text{(A-12)}$$

One can now use the transversality conditions, Eqs (57), to solve for the three constants. Equating the transversality conditions to Eqs (A-10), (A-11) and (A-12) at $\tau = \tau_f$ gives

$$2Y_{1f} = C_1 + 3P_3\tau_f + C_2 \sin\tau_f + C_3 \cos\tau_f \qquad \text{(A-13)}$$

$$0 = -2P_3 - C_2 \cos\tau_f + C_3 \sin\tau_f \qquad \text{(A-14)}$$

$$0 = C_1 + 3P_3\tau_f + 2C_2 \sin\tau_f + 2C_3 \cos\tau_f \qquad \text{(A-15)}$$

Subtract Eq (A-15) from twice Eq (A-13) to yield

$$4Y_{1f} = C_1 + 3P_3\tau_f$$

or

$$C_1 = 4Y_{1f} - 3P_3\tau_f \qquad \text{(A-16)}$$

Substitute Eq (A-16) into Eq (A-15):

$$0 = 4Y_{1f} - 3P_3\tau_f + 3P_3\tau_f + 2C_2 \sin \tau_f + 2C_3 \cos \tau_f$$

$$= 2Y_{1f} + C_2 \sin \tau_f + C_3 \cos \tau_f \qquad \text{(A-17)}$$

Solving Eq (A-14) for C_2

$$C_2 = - \frac{2P_3}{\cos \tau_f} + C_3 \tan \tau_f \qquad \text{(A-18)}$$

Substitute Eq (A-18) into Eq (A-17) to get

$$0 = 2Y_{1f} - 2P_3 \tan \tau_f + \frac{C_3 \sin^2 \tau_f}{\cos \tau_f} + C_3 \cos \tau_f$$

Multiplying each term by $\cos \tau_f$,

$$0 = 2Y_{1f} \cos \tau_f - 2P_3 \sin \tau_f + C_3$$

Thus,

$$C_3 = 2P_3 \sin \tau_f - 2Y_{1f} \cos \tau_f \qquad \text{(A-19)}$$

Substitute Eq (A-19) into Eq (A-18):

$$C_2 = - \frac{2P_3}{\cos \tau_f} + 2P_3 \frac{\sin^2 \tau_f}{\cos \tau_f} - 2Y_{1f} \sin \tau_f$$

$$= - 2P_3 \cos \tau_f - 2Y_{1f} \sin \tau_f \qquad \text{(A-20)}$$

One can now use the values of these constants to form the following closed form expressions for the costates:

$$P_1 = 4Y_{1f} + 3P_3(\tau-\tau_f) - 2P_3 \cos\tau_f \sin\tau - 2Y_{1f} \sin\tau_f \sin\tau$$

$$+ 2P_3 \sin\tau_f \cos\tau - 2Y_{1f} \cos\tau_f \cos\tau$$

$$= 4Y_{1f} - 3P_3(\tau_f-\tau) + 2P_3 \sin(\tau_f-\tau) - 2Y_{1f} \cos(\tau_f-\tau)$$

$$= 4Y_{1f} - 6Y_{3f}(\tau_f-\tau) + 4Y_{3f} \sin(\tau_f-\tau)$$

$$- 2Y_{1f} \cos(\tau_f-\tau) \qquad \text{(A-21)}$$

$$P_2 = -2P_3 + 2P_3 \cos\tau_f \cos\tau + 2Y_{1f} \sin\tau_f \cos\tau$$

$$+ 2P_3 \sin\tau_f \sin\tau - 2Y_{1f} \cos\tau_f \sin\tau$$

$$= -2P_3 + 2P_3 \cos(\tau_f-\tau) + 2Y_{1f} \sin(\tau_f-\tau)$$

$$= -4Y_{3f} + 4Y_{3f} \cos(\tau_f-\tau) + 2Y_{1f} \sin(\tau_f-\tau) \qquad \text{(A-22)}$$

From before,

$$P_3 = 2Y_{3f} \qquad \text{(A-1)}$$

Lastly,

$$P_4 = 4Y_{1f} - 3P_3\tau_f + 3P_3\tau - 4P_3 \cos\tau_f \sin\tau$$

$$- 4Y_{1f} \sin\tau_f \sin\tau + 4P_3 \sin\tau_f \cos\tau - 4Y_{1f} \cos\tau_f \cos\tau$$

$$= 4Y_{1f} - 3P_3 (\tau_f-\tau) - 4Y_{1f} \cos(\tau_f-\tau) + 4P_3 \sin(\tau_f-\tau)$$

$$= 4Y_{1f} - 6Y_{3f} (\tau_f-\tau) - 4Y_{1f} \cos(\tau_f-\tau)$$

$$+ 8Y_{3f} \sin(\tau_f-\tau) \qquad \text{(A-23)}$$

Thus, the costates are functions only of the terminal states and the time to go. This implies that the control angle, which is a function of only the costates, is also a function only of the terminal states and the time to go.

Appendix B

Non-linear Trajectories

This appendix displays in Figs. 21 through 26 the actual optimum non-linear trajectories defined in Chapter IV, Table I. In each run, the pursuer (△) is at a higher altitude than the evader (□) and the pursuer has a greater final velocity than the evader. The position angle THETA is measured from the position at the final time.

These trajectories were generated by assuming the final states and integrating backward in time as discussed in Chapter IV. Those final states were also given in Chapter IV. Other constants used in these simulations, but which are only incidental to this study, are listed below:

Vehicles' weight	10,000 lb.
Pursuer's thrust	500 lb.
Evader's thrust	100 lb.
Vehicles' I_{sp}	300 sec.

It has been assumed that the mass of each vehicle is constant. Actually, in a real case, mass (m) would be changing by the expression

$$m = M_0 + \dot{m}\Delta t$$

where M_0 is the initial mass, $\dot{m}$ is the propellant flow rate and Δt the burn time. The accuracy of the constant mass assumption lies in the magnitude of the $\dot{m}\Delta t$ term. The smaller this term in relation to M_0, the better the assumption.

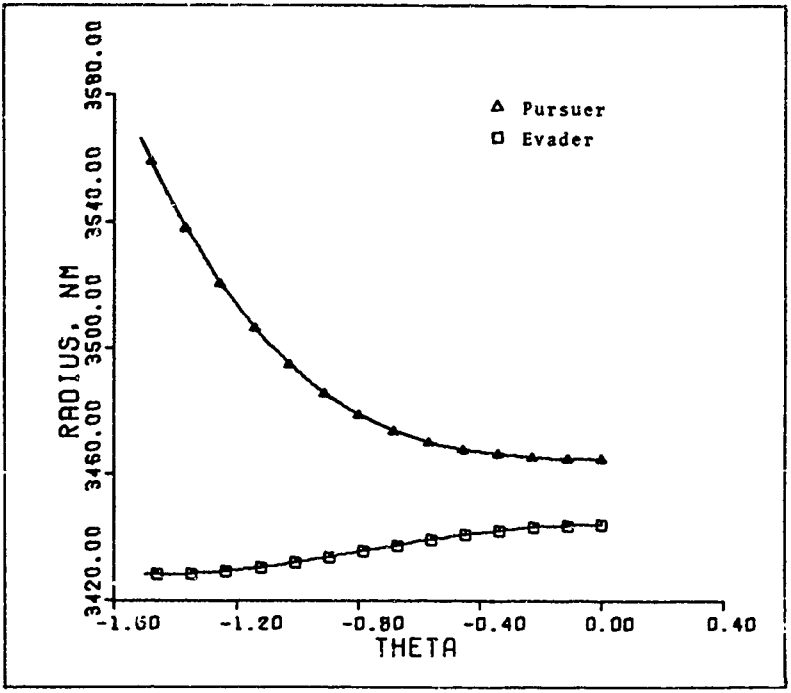

Fig. 21. Optimum Pursuer and Evader Trajectories in terms of Earth Central Angle (Radians) and Radius, Non-linear Run 1.

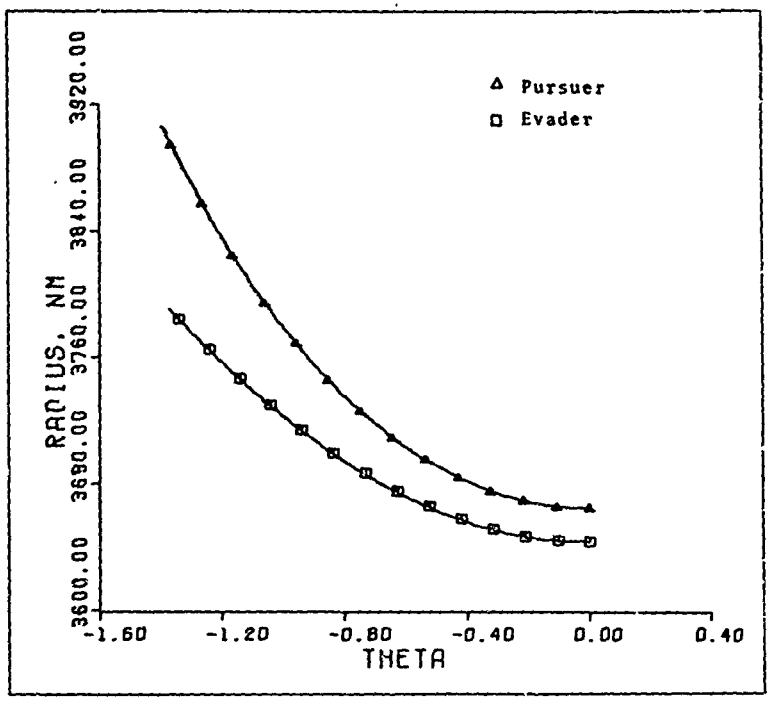

Fig. 22. Optimum Pursuer and Evader Trajectories in terms of Earth Central Angle (Radians) and Radius, Non-linear Run 2.

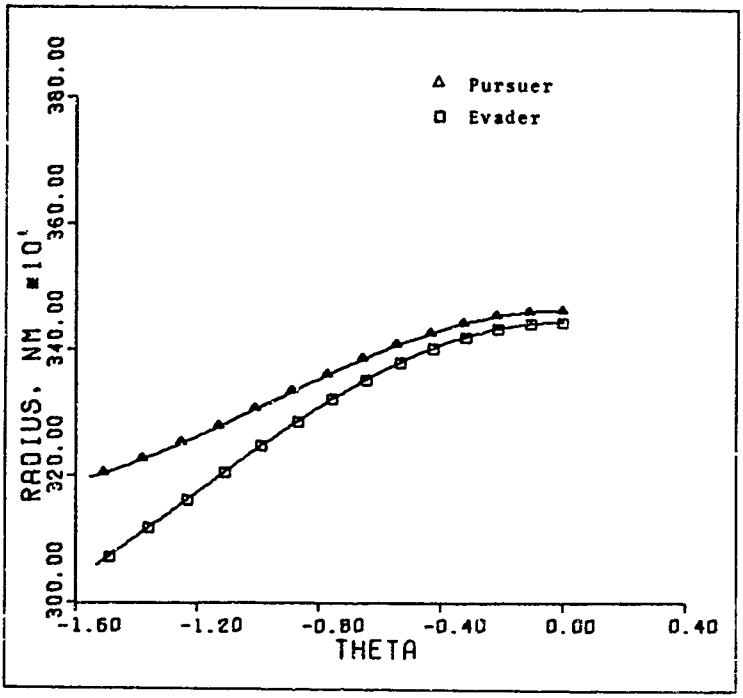

Fig. 23. Optimum Pursuer and Evader Trajectories in terms of Earth Central Angle (Radians) and Radius, Non-linear Run 3.

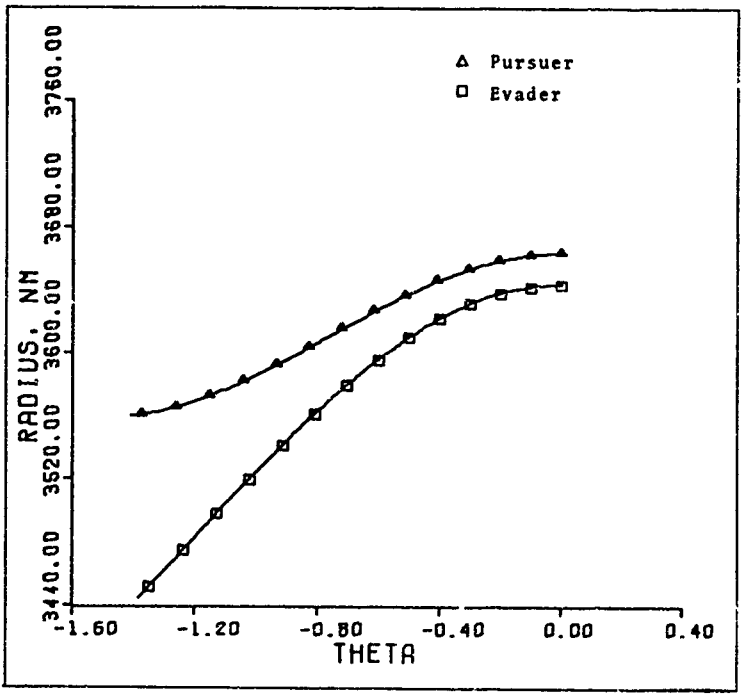

Fig. 24. Optimum Pursuer and Evader Trajectories in terms of Earth Central Angle (Radians) and Radius, Non-linear Run 4.

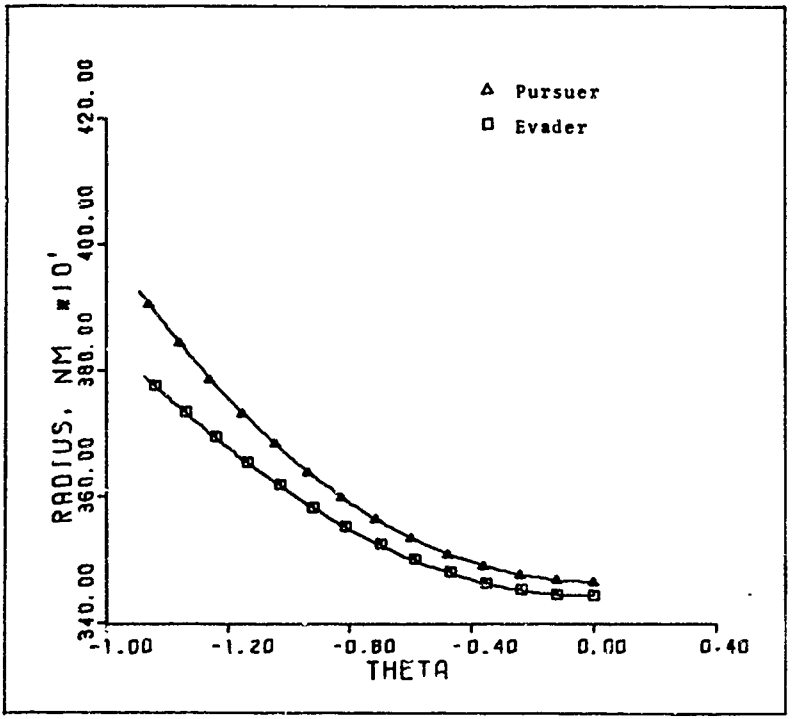

Fig. 25. Optimun Pursuer and Evader Trajectories in terms of Earth Central Angle (Radians) and Radius, Non-linear Run 5.

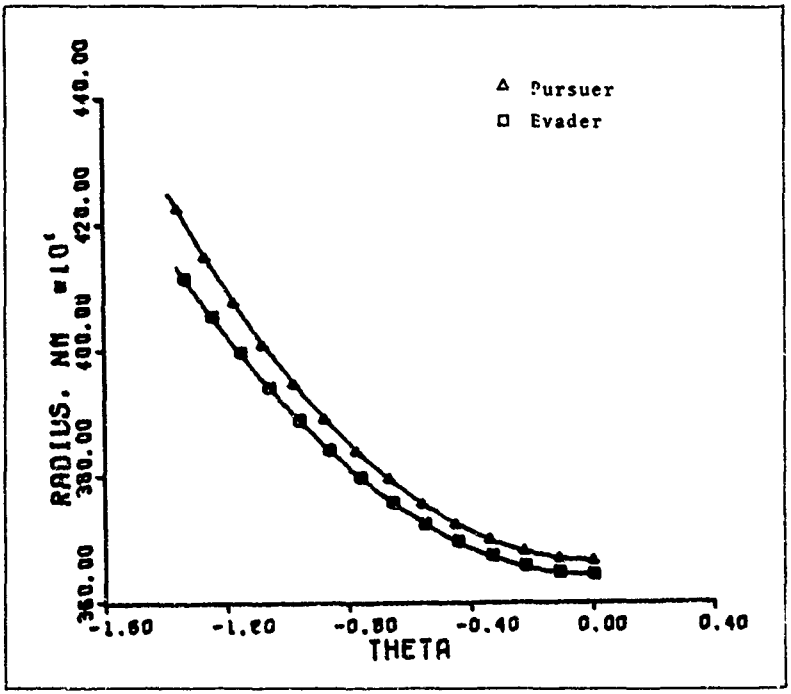

Fig. 26. Optimum Pursuer and Evader Trajectories in terms of Earth Central Angle (Radians) and Radius, Non-linear Run 6.

For this study, M_0 = 10,000 lb/g = 310 lb sec^2/ft while $\dot{m} = \frac{-T}{gI_{sp}}$ = -0.0517 lb sec/ft for the pursuer and five times less for the evader. Thus, each hundred seconds of burn time would decrease the pursuer's mass by only 5.17 lb sec^2/ft, or roughly only 0.2%. Thus, it is felt that the assumption of constant mass is justified for this study.

Also shown in this appendix are the values of the non-linear separation distance between the vehicles as a function of time. Again, time is measured relative to the final time. Thus, time is actually time to go. It can be seen that the plots are all very similar.

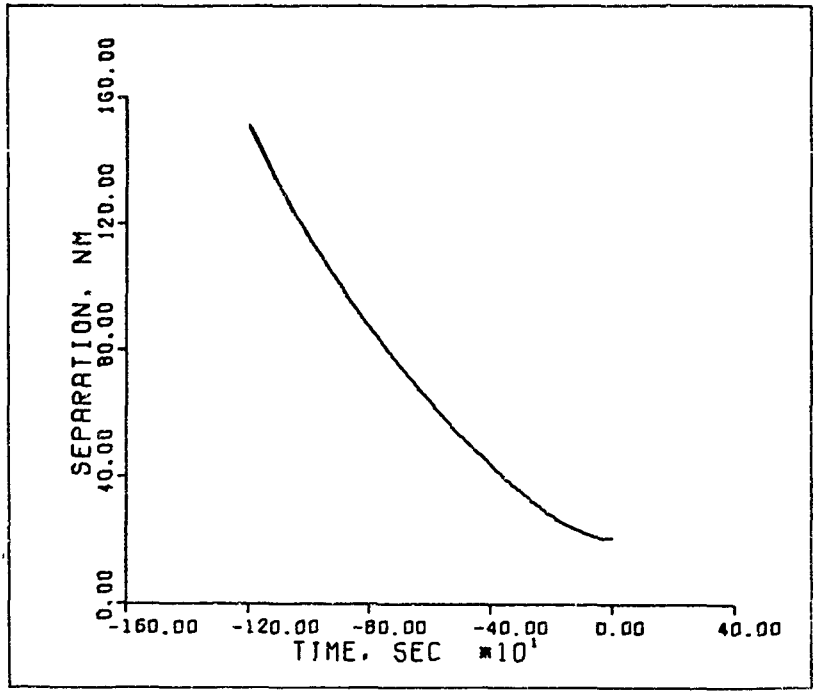

Fig. 27. Time History of Vehicle Separation Distance for Optimum Non-linear Trajectory Run 1.

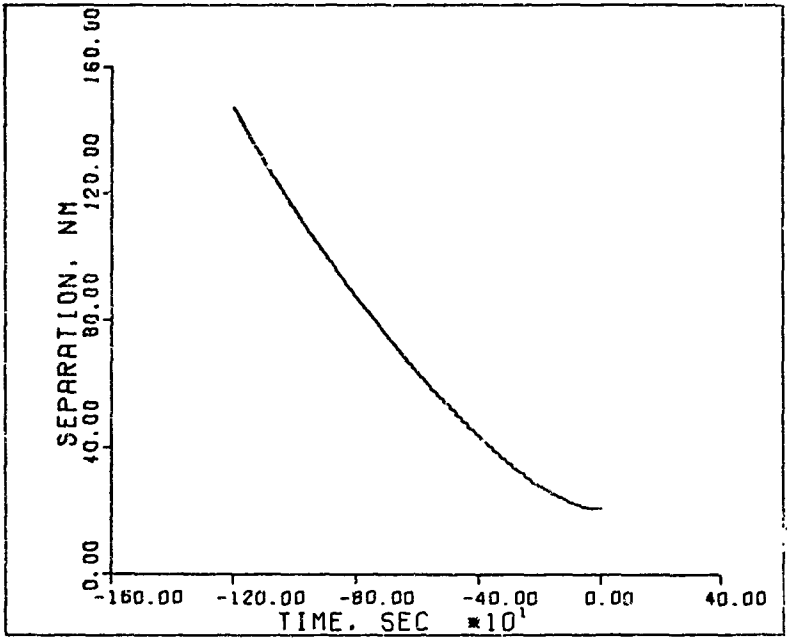

Fig. 28. Time History of Vehicle Separation Distance for Optimum Non-linear Trajectory Run 2.

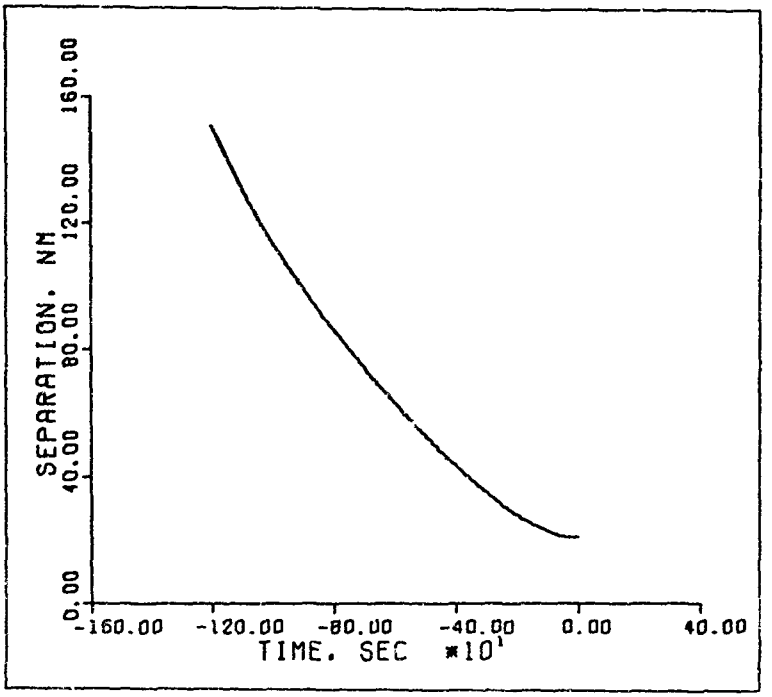

Fig. 29. Time History of Vehicle Separation Distance for Optimum Non-linear Trajectory Run 3.

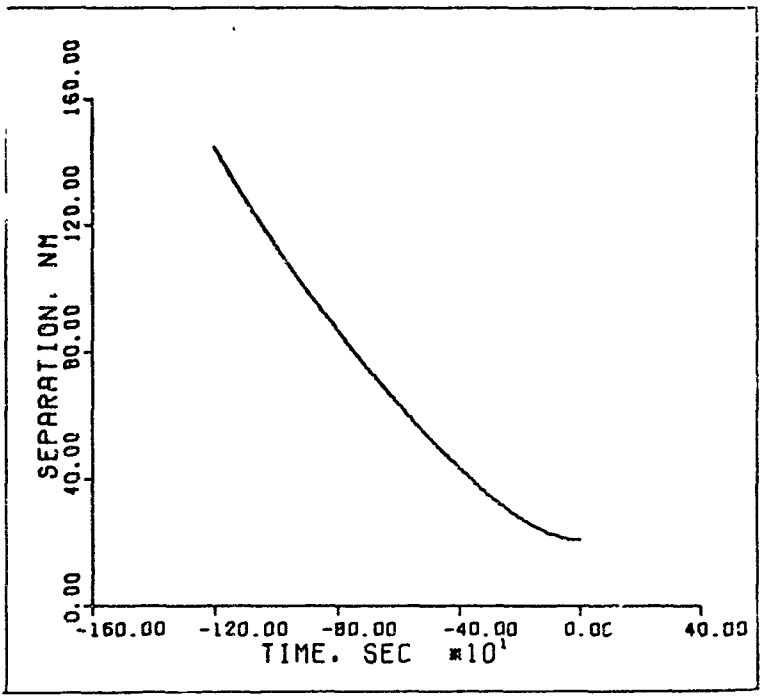

Fig. 30. Time History of Vehicle Separation Distance for Optimum Non-linear Trajectory Run 4.

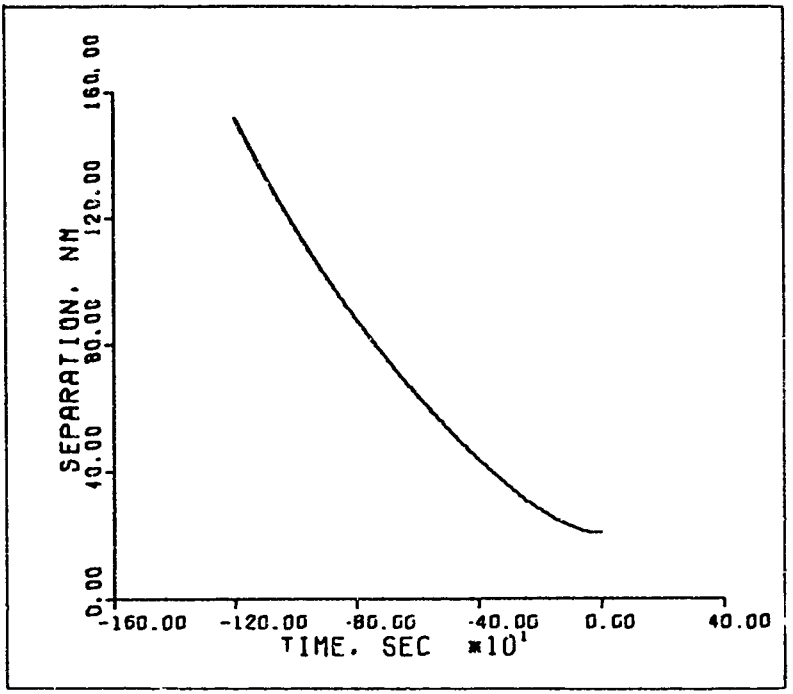

Fig. 31. Time History of Vehicle Separation Distance for Optimum Non-linear Trajectory Run 5.

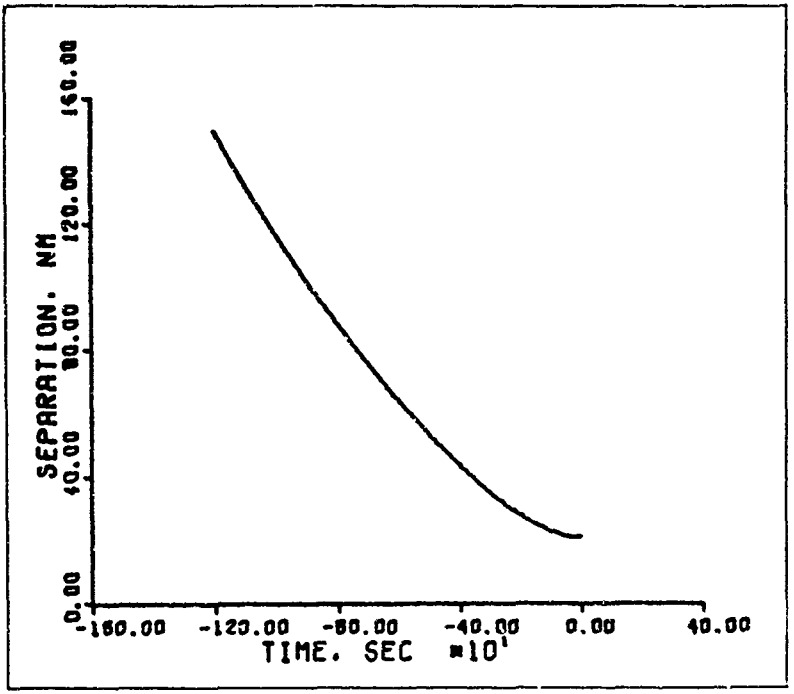

Fig. 32. Time History of Vehicle Separation Distance for Optimum Non-linear Trajectory Run 6.

Appendix C

Discussion of Computer Solutions to the TPBVP's

This appendix discusses some of the computational aspects of the solutions to the TPBVP's discussed in Chapter V. All computer analysis was done on a CDC 3600 computer system with a Calcomb plotting device.

Fixed-time Solutions

As was discussed in Chapter V, three points from each of the six backward generated non-linear trajectories were used as input data. Please note that as fixed-time solutions it was assumed that the time to go corresponding to the input data was known.

Since the program used actually attempts to converge to the initial (or input) data, the convergence accuracy desired relates directly to the real computer time required for this convergence. The runs shown in Chapter V were required to converge to within 0.0001 of the input values. CDC 3600 computer processing time corresponded almost directly to 180 seconds per characteristic time unit. That is, to converge to input from 1.0 characteristic time units from the terminal state required 180 seconds of computer time. Likewise, the data at $(\tau-\tau_f) = -0.5$ took about 90 seconds and the data at $(\tau-\tau_f) = -0.25$ took on the order of 45 seconds. Since one characteristic time unit is equal to about 806 actual seconds, the above discussion implies that given a

set of initial conditions, the fixed-time TPBVP would be solved (converged to within 0.0001 of initial conditions) in approximately 22% of the remaining time to go. This solution time could be decreased with the allowance of looser tolerances, or with the use of special purpose computers.

Free-time Solutions

Since in the free-time problem, the actual time to go corresponding to the initial conditions was not known, a somewhat arbitrary value was assumed. A fixed-time solution was then generated to fit this particular time to go. The final range squared rate for this solution was calculated. Then the estimate of time to go was iterated upon to drive the final range squared rate to zero. Hence, as discussed in Chapter V, the free-time solution simply selected that fixed-time solution which corresponded to the minimum final separation distance.

By viewing the free-time solutions shown in Chapter V, it will be noted that in all cases the solution for time to go is shorter than the actual time to go. This is because the initial estimate of time to go was selected to be smaller, as discussed before, than the actual value and the program then increases that value until the terminal range squared rate was within some tolerance of zero. The curves shown required that tolerance to be 10^{-5}. A few runs were attempted using 10^{-6}, but the convergence had not occurred after 50% of the time to go had passed.

Also important is the desired accuracy with which the solution meets the given (measured) initial states. Remember for the fixed-time solutions, the program was forced to meet these states within 0.0001. Since each free-time solution actually involves several fixed-time solutions, to keep the overall convergence time to within acceptable limits this 0.0001 tolerance had to be increased. After several tries, it was found that 0.002 would work with fairly acceptable results. That value, then, is the one that was used to generate the solutions in this study.

Appendix D

Transition Matrix Derivation

This appendix will derive the individual terms that comprise the transition matrix Φ discussed in Chapter VII. From the theory of linear equations,

$$\frac{d}{d\tau}\left[\Phi(\tau_f,\tau)\right]^T = -[F(\tau)]^T[\Phi(\tau_f,\tau)]^T \qquad \text{(D-1)}$$

with the boundary condition

$$[\Phi(\tau_f,\tau_f)] = [I] \qquad \text{(D-2)}$$

where I represents the identity matrix. From Chapter VI, F has been determined to be a constant matrix:

$$[F] = \begin{bmatrix} 0 & 1 & 0 & 0 \\ 1 & 0 & 0 & 2 \\ -1 & 0 & 0 & 1 \\ 0 & -1 & 0 & 0 \end{bmatrix}$$

Thus, Eq (D-1) is equivalent to

$$\begin{bmatrix} \phi'_{11} & \phi'_{12} & \phi'_{13} & \phi'_{14} \\ \phi'_{21} & \phi'_{22} & \phi'_{23} & \phi'_{24} \\ \phi'_{31} & \phi'_{32} & \phi'_{33} & \phi'_{34} \\ \phi'_{41} & \phi'_{42} & \phi'_{43} & \phi'_{44} \end{bmatrix} = -\begin{bmatrix} \phi'_{11} & \phi'_{12} & \phi'_{13} & \phi'_{14} \\ \phi'_{21} & \phi'_{22} & \phi'_{23} & \phi'_{24} \\ \phi'_{31} & \phi'_{32} & \phi'_{33} & \phi'_{34} \\ \phi'_{41} & \phi'_{42} & \phi'_{43} & \phi'_{44} \end{bmatrix} \begin{bmatrix} 0 & 1 & 0 & 0 \\ 1 & 0 & 0 & 2 \\ -1 & 0 & 0 & 1 \\ 0 & -1 & 0 & 0 \end{bmatrix}$$

$$= \begin{bmatrix} (\phi_{13}-\phi_{12}) & (\phi_{14}-\phi_{11}) & 0 & (-\phi_{13}-2\phi_{12}) \\ (\phi_{23}-\phi_{22}) & (\phi_{24}-\phi_{21}) & 0 & (-\phi_{23}-2\phi_{22}) \\ (\phi_{33}-\phi_{32}) & (\phi_{34}-\phi_{31}) & 0 & (-\phi_{33}-2\phi_{32}) \\ (\phi_{43}-\phi_{42}) & (\phi_{44}-\phi_{41}) & 0 & (-\phi_{43}-2\phi_{42}) \end{bmatrix} \qquad \text{(D-3)}$$

which is actually sixteen equations while Eq (D-2) provides sixteen boundary conditions at the final time. Since the third column in the right hand side of Eq (D-3) consists only of zeros, the terms corresponding to those parameters (ϕ_{13}, ϕ_{23}, ϕ_{33} and ϕ_{43}) are all simply constants that do not vary with time. Utilizing the boundary conditions, those constants are seen to be

$$\phi_{13} = 0 \qquad \text{(D-4a)}$$

$$\phi_{23} = 0 \qquad \text{(D-4b)}$$

$$\phi_{33} = 1 \qquad \text{(D-4c)}$$

$$\phi_{43} = 0 \qquad \text{(D-4d)}$$

Now from Eq (D-3)

$$\phi'_{11} = -\phi_{12}$$

$$\phi''_{11} = -\phi'_{12}$$

$$= -\phi_{14} + \phi_{11}$$

$$\dot{\phi}_{11}''' = -\phi_{14}' + \phi_{11}'$$

$$= 2\phi_{12} + \phi_{11}'$$

$$= -\phi_{11}'$$

or

$$\phi_{11}''' + \phi_{11}' = 0$$

Normally, the solution to the above expression would involve terms like cos τ and sin τ. However, with the aid of hindsight and the form of the solutions in Appendix A, let the solution here be written in terms of $\tau_f - \tau$, or $\Delta\tau$

$$\phi_{11} = A_{11} + B_{11} \sin \Delta\tau + C_{11} \cos \Delta\tau$$

$$\phi_{11}(\tau_f) = A_{11} + C_{11}$$

$$= 1$$

or

$$A_{11} = 1 - C_{11}$$

Thus

$$\phi_{11}(\tau) = 1 - C_{11} + B_{11} \sin \Delta\tau + C_{11} \cos \Delta\tau$$

$$= 1 + B_{11} \sin \Delta\tau + C_{11}(\cos \Delta\tau - 1) \qquad \text{(D-5a)}$$

Again from Eq (D-3),

$$\phi'_{21} = -\phi_{22}$$

$$\phi''_{21} = -\phi'_{22}$$

$$= -\phi_{24} + \phi_{21}$$

$$\phi'''_{21} = -\phi'_{24} + \phi'_{21}$$

$$= 2\phi_{22} + \phi'_{21}$$

$$= -2\phi'_{21} + \phi'_{21}$$

$$= -\phi'_{21}$$

or

$$\phi'''_{21} + \phi'_{21} = 0$$

As before, let

$$\phi_{21} = A_{21} + B_{21} \sin \Delta\tau + C_{21} \cos \Delta\tau$$

$$\phi_{21}(\tau_f) = A_{21} + C_{21}$$

$$= 0$$

or

$$A_{21} = -C_{21}$$

Thus,

$$\phi_{21}(\tau) = B_{21} \sin \Delta\tau + C_{21}(\cos \Delta\tau - 1) \quad \text{(D-5b)}$$

Again from Eq (D-3),

$$\phi'_{31} = 1 - \phi_{32}$$

$$\phi''_{31} = -\phi'_{32}$$

$$= \phi_{31} - \phi_{34}$$

$$\phi'''_{31} = \phi'_{31} - \phi'_{34}$$

$$= \phi'_{31} + 1 + 2\phi_{32}$$

$$= \phi'_{31} + 1 + 2 - 2\phi'_{31}$$

$$= 3 - \phi'_{31}$$

or

$$\phi'''_{31} = \phi'_{31} = 3$$

Let

$$\phi_{31} = A_{31} + B_{31} \sin \Delta\tau + C_{31} \cos \Delta\tau - 3\Delta\tau$$

$$\phi_{31}(\tau_f) = A_{31} + C_{31}$$

$$= 0$$

or

$$A_{31} = -C_{31}$$

Thus,

$$\phi_{31} = B_{31} \sin \Delta\tau + C_{31}(\cos \Delta\tau - 1) - 3\Delta\tau \qquad \text{(D-5c)}$$

Back to Eq (D-3) for

$$\phi'_{41} = -\phi_{42}$$

$$\phi''_{41} = -\phi'_{42}$$

$$= \phi_{41} - \phi_{44}$$

$$\phi'''_{41} = \phi'_{41} - \phi'_{44}$$

$$= \phi'_{41} + 2\phi_{42}$$

$$= \phi'_{41} - 2\phi'_{41}$$

$$= -\phi'_{41}$$

or

$$\phi'''_{41} + \phi'_{41} = 0$$

whose solution is

$$\phi_{41} = A_{41} + B_{41} \sin \Delta\tau + C_{41} \cos \Delta\tau$$

$$\phi_{41}(\tau_f) = A_{41} + C_{41}$$

$$= 0$$

or

$$A_{41} = -C_{41}$$

Thus,

$$\phi_{41} = B_{41} \sin \Delta\tau + C_{41}(\cos \Delta\tau - 1) \quad \text{(D-5d)}$$

Now, beginning the second column of the transition matrix

$$\phi_{12} = -\phi'_{11}$$

$$= B_{11} \cos \Delta\tau - C_{11} \sin \Delta\tau$$

$$\phi_{12}(\tau_f) = B_{11}$$

$$= 0$$

Thus

$$\phi_{12} = -C_{11} \sin \Delta\tau \qquad \text{(D-6a)}$$

and

$$\phi_{11} = 1 + C_{11}(\cos \Delta\tau - 1) \qquad \text{(D-6b)}$$

Also,

$$\phi_{22} = -\phi'_{21}$$

$$= B_{21} \cos \Delta\tau - C_{21} \sin \Delta\tau$$

$$\phi_{22}(\tau_f) = B_{21}$$

$$= 1$$

Thus,

$$\phi_{22} = \cos \Delta\tau - C_{21} \sin \Delta\tau \qquad \text{(D-6c)}$$

$$\phi_{21} = \sin \Delta\tau + C_{21} \cos \Delta\tau \qquad \text{(D-6d)}$$

Also,

$$\phi_{32} = 1 - \phi'_{31}$$

$$= -2 + B_{31} \cos \Delta\tau - C_{31} \sin \Delta\tau$$

$$\phi_{32}(\tau_f) = -2 + B_{31}$$

$$= 0$$

or

$$B_{31} = 2$$

Thus,

$$\phi_{32} = 2 \cos \Delta\tau - C_{31} \sin \Delta\tau - 2 \qquad \text{(D-6e)}$$

and

$$\phi_{31} = 2 \sin \Delta\tau + C_{31} (\cos \Delta\tau - 1) - 3\Delta\tau \qquad \text{(D-3f)}$$

Also,

$$\phi_{42} = -\phi'_{41}$$

$$= B_{41} \cos \Delta\tau - C_{41} \sin \Delta\tau$$

$$\phi_{42}(\tau_f) = B_{41}$$

$$0$$

Thus,

$$\phi_{42} = -C_{41} \sin \Delta\tau \qquad \text{(D-6g)}$$

and

$$\phi_{41} = C_{41} (\cos \Delta\tau - 1) \qquad \text{(D-6h)}$$

Also

$$\phi_{14} = \phi'_{12} + \phi_{11}$$

$$= C_{11} \cos \Delta\tau + 1 + C_{11} \cos \Delta\tau - C_{11}$$

$$= 2C_{11} \cos \Delta\tau + 1 - C_{11}$$

$$\phi_{14}(\tau_f) = 2C_{11} + 1 - C_{11}$$

$$= C_{11} + 1$$

$$= 0$$

or

$$C_{11} = -1$$

Thus

$$\phi_{14} = -2 \cos \Delta\tau + 2 \qquad \text{(D-7a)}$$

and from Eq (D-6a),

$$\phi_{12} = \sin \Delta\tau \qquad \text{(D-7b)}$$

From Eq (D-6b),

$$\phi_{11} = 1 - (\cos \Delta\tau - 1)$$

$$= 2 - \cos \Delta\tau \qquad \text{(D-7c)}$$

Again from Eq (D-3),

$$\phi_{24} = \phi'_{22} + \phi'_{21}$$

$$= \sin \Delta\tau + C_{21} \cos \Delta\tau + \sin \Delta\tau + C_{21} \cos \Delta\tau - C_{21}$$

$$= 2 \sin \Delta\tau + 2 C_{21} \cos \Delta\tau - C_{21} \qquad \text{(D-8)}$$

$$\phi_{24}(\tau_f) = 2C_{21} - C_{21}$$

$$= C_{21}$$

$$= 0$$

Thus

$$\phi_{24} = 2 \sin \Delta\tau \qquad \text{(D-9a)}$$

Also, from Eq (E-6c),

$$\phi_{22} = \cos \Delta\tau \qquad \text{(D-9b)}$$

From Eq (E-6d),

$$\phi_{21} = \sin \Delta\tau \qquad \text{(D-9c)}$$

Once more using the original expression from Eq (D-3),

$$\phi_{34} = \phi'_{32} + \phi_{31}$$

$$= 2 \sin \Delta\tau + C_{31} \cos \Delta\tau + 2 \sin \Delta\tau + C_{31} \cos \Delta\tau - C_{31} - 3\Delta\tau$$

$$= 4 \sin \Delta\tau + 2C_{31} \cos \Delta\tau - C_{31} - 3\Delta\tau \qquad \text{(D-10)}$$

$$\phi_{34}(\tau_f) = 2C_{31} - C_{31}$$

$$= C_{31}$$

$$= 0$$

Thus

$$\phi_{34} = 4 \sin \Delta\tau - 3\Delta\tau \qquad \text{(D-11a)}$$

and from Eq (D-6e),

$$\phi_{32} = 2 \cos \Delta\tau - 2 \qquad \text{(D-11b)}$$

and from Eq (D-6f),

$$\phi_{31} = 2 \sin \Delta\tau - 3\Delta\tau \qquad \text{(D-11c)}$$

Now, lastly from Eq (D-3),

$$\phi_{44} = \phi'_{42} + \phi_{41}$$

$$= C_{41} \cos \Delta\tau + C_{41} \cos \Delta\tau - C_{41}$$

$$= 2C_{41} \cos \Delta\tau - C_{41} \qquad \text{(D-12)}$$

$$\phi_{44}(\tau_f) = 2C_{41} - C_{41}$$

$$= C_{41}$$

$$= 1$$

Thus,

$$\phi_{44} = 2 \cos \Delta\tau - 1 \qquad \text{(D-13a)}$$

and from Eq (D-6g),

$$\phi_{42} = - \sin \Delta\tau \qquad \text{(D-13b)}$$

From Eq (D-6h),

$$\phi_{41} = \cos \Delta\tau - 1 \qquad \text{(D-13c)}$$

And now, finally, Eqs (D-4), (D-7), (D-9), (D-11) and (D-13) constitute the solution to the transition matrix. Thus

$$[\phi] = \begin{bmatrix} (2 - \cos \Delta\tau) & (\sin \Delta\tau) & 0 & (2 - 2 \cos \Delta\tau) \\ (\sin \Delta\tau) & (\cos \Delta\tau) & 0 & (2 \sin \Delta\tau) \\ (2 \sin \Delta\tau - 3\Delta\tau) & (2 \cos \Delta\tau - 2) & 1 & (4 \sin \Delta\tau - 3\Delta\tau) \\ (\cos \Delta\tau - 1) & (-\sin \Delta\tau) & 0 & (2 \cos \Delta\tau - 1) \end{bmatrix}$$

Vita

Richard H. Woodward was born on 5 October 1944 in Ottumwa, Iowa. He was graduated from Ottumwa High School in 1962 and then attended Iowa State University. During his study there he participated in an engineering co-op program which allowed him to spend one year at NASA's Flight Research Center, Edwards Air Force Base where he was assigned to the X-15 test program. Upon graduation in 1967 with a Bachelor of Science degree in Aerospace Engineering he also received a commission in the USAF. He was then assigned to the Military Space Systems Branch of the Foreign Technology Division (AFSC) at Wright-Patterson Air Force Base, Ohio. In June 1970 he entered the Graduate Astronautics program at the Air Force Institute of Technology School of Engineering.

This thesis was typed by Jane Manemann.